

external jugular vein and the right common carotid artery in the recipients were dissected, mobilized and fixed to the appropriate cuffs. The cuffs were composed of polyethylene tubes (2.5F; Portex Co. Ltd., London, United Kingdom). The aorta and the main pulmonary artery of the harvested donor heart were drawn over the end of the common carotid artery and the external jugular vein for anastomoses. The grafts were monitored by daily inspection and palpation. Rejection was determined by the cessation of beating of the graft and was confirmed by histology.

3.7. Statistical analyses

Data are presented as mean \pm S.E.M. Statistical differences of the results among the experimental groups were calculated using one-way ANOVA. A value of $p < 0.05$ was accepted as statistically significant.

4. Results

4.1. Induction of endotoxin tolerance by pretreatment with low doses of LPS

Prior to the challenge with a high dose of LPS, the mice were treated with low doses of LPS twice, in order to induce ET. The survival rate at 72 h after challenging with a high dose of LPS showed a dramatically improved in mice by pretreatment with low doses of LPS (100%, $n=6$). In contrast, the survival curve of the control mice that were challenged with a high dose of LPS without pretreatment had a steep slope (survival rate at 72 h = 0%, $n=6$). All the endotoxin-tolerized mice were not immobile; they exhibited shivering and diarrhea even after the challenge with a high dose of LPS. However, the high dose LPS challenge caused septic syndrome in the control mice.

4.2. The time course of the endotoxin-tolerized B6 mouse heart rejection was significantly slower than that of the untreated B6 mouse heart rejection in BALB/c mice

In order to determine whether the induction of ET in donor animals prior to harvesting organ grafts would have a prolonged effect on the graft survival in allogeneic recipients, the hearts of B6 mice that were treated with either only low doses of LPS (protocol 1) or low doses of LPS followed by a high dose of LPS (protocol 2), and then transplanted into BALB/c mice. The control hearts from PBS-treated B6 mice were also transplanted into BALB/c mice. In the absence of any immunosuppressive therapy, the median survival time of the hearts from B6 mice treated with protocols 1 and 2 were 9 and 16 days, respectively, whereas that of the control hearts transplanted into BALB/c mice was 8 days (Fig. 1). Thus, the survival of the heart allografts was significantly prolonged if the organ was obtained from endotoxin-tolerized mice that were prepared by challenging the mice with a low dose LPS followed by a high dose LPS.

4.3. Splenocytes from B6 mice that had been rendered endotoxin tolerant had lowered allogeneic T cell stimulation ability

In order to evaluate the capacity of splenocytes from endotoxin-tolerized mice to stimulate allogeneic T cells, the MLR assay was performed using irradiated splenocytes from either PBS-injected control or LPS-treated B6 mice as stimulators and CFSE-labeled splenocytes from BALB/c mice as responders. When the splenocytes from the control mice were used as stimulators, a remarkable proliferation of allogeneic CD4⁺ and CD8⁺ T cells was observed. In contrast, such a proliferation of allogeneic CD4⁺ and CD8⁺ T cells was sup-

pressed when splenocytes from LPS-treated mice were used as stimulators (Fig. 2A). The SI of allogeneic CD4⁺ and CD8⁺ T cells in response to the splenocyte stimulators from LPS-treated mice was significantly lower than those in response to the splenocyte stimulators from control mice (Fig. 2B). Protocol 2 induced more profound suppressive effects on allostimulation than protocol 1. Thus, treating a transplant donor with a low dose of LPS followed by challenge with a high dose of LPS inhibits the capacity of the donor's APCs to stimulate allogeneic T cells.

4.4. DCs from the endotoxin-tolerized mice significantly altered the expression of molecules necessary for antigen presentation

The impaired stimulation of allogeneic T cell proliferation in the splenocyte stimulators from endotoxin-tolerized mice might be due to their incompetence in presenting alloantigens. To address this possibility, the phenotypical alterations in DCs, which are the predominant APCs among splenocytes, were analyzed after the LPS treatments. The method of staining with a combination of CD11c and CD11b was used to separate the myeloid-related and lymphoid-related DCs in the splenocytes (Fig. 3A). CD11c⁺ CD11b⁺ is the phenotype of myeloid-related DCs, residing in the marginal zones of the spleen [16,17]. In our study, the CD11c⁺ CD11b⁺ subset was further divided into CD11c^{int} CD11b⁺ and CD11c^{bright} CD11b⁺ subsets; this probably reflects the difference in maturation. Cells from the control mice belonging to the CD11c^{bright} CD11b⁺ subset expressed all the molecules necessary for effective T cell stimulation (MHC class II, CD40, CD80 and CD86), thus indicating their maturity (Fig. 3B). LPS treatments—using protocols 1 or 2—did not affect the percentage of CD11c^{bright} CD11b⁺ DCs; instead it reduced the expression level of MHC class II molecules on this subset (Fig. 3C). The CD11c^{int} CD11b⁺ subset in the spleen of control mice comprised class II^{dim} CD40⁺ CD80⁺ immature DCs and class II^{bright} CD40⁺ CD80⁺ mature DCs. LPS treatments resulted in the expansion of the CD11c^{int} CD11b⁺ subset and increased the proportion of mature DCs in this subset (Fig. 3B). In addition, the expression level of MHC class II molecules on mature DCs in the CD11c^{int} CD11b⁺ subset of the splenocytes from LPS-treated mice was significantly higher than that of the splenocytes from the control mice (Fig. 3C). CD11c⁺ CD11b[−] is the phenotype of lymphoid-related DCs, which reside in the T cell zones [16,17]. Further, the CD11c⁺ CD11b[−] subset comprised class II^{dim} CD40^{dim} immature DCs and class II^{bright} CD40⁺ mature DCs. In contrast to the CD11b⁺ myeloid-related DC subset, the LPS treatments resulted in a decreased proportion of mature DCs in the CD11b[−] lymphoid-related DC subset, i.e., reduction of class II^{bright} CD40⁺ DCs (Fig. 3B). In addition, the expression level of MHC class II molecules on mature DCs in the CD11c⁺ CD11b[−] subset of the splenocytes from LPS-treated mice was significantly lower than that of the splenocytes from the control mice (Fig. 3C). Such LPS-induced modulations on the lymphoid-related DCs by protocol 2 were more notable than those induced by protocol 1. Thus, the induction of ET increased the proportion of myeloid-related DCs expressing molecules necessary for antigen presentation, but reduced the proportion of lymphoid-related DCs expressing these molecules.

4.5. DCs from the endotoxin-tolerized mice showed up-regulation of FasL expression on their cell surface

It has been demonstrated that the expression of FasL molecules are induced in well-developed mature DCs; Fas–FasL interactions usually lead to the apoptosis-induced cell death of antigen-primed T cells [18]. This may be a regulatory mechanism to curb the excessive adaptive

immune responses of T cells. As shown in Fig. 4, LPS treatment using protocol 2 significantly increased FasL expression on the surface of splenic DCs, particularly on the CD11c⁺ CD11b⁺ myeloid-related

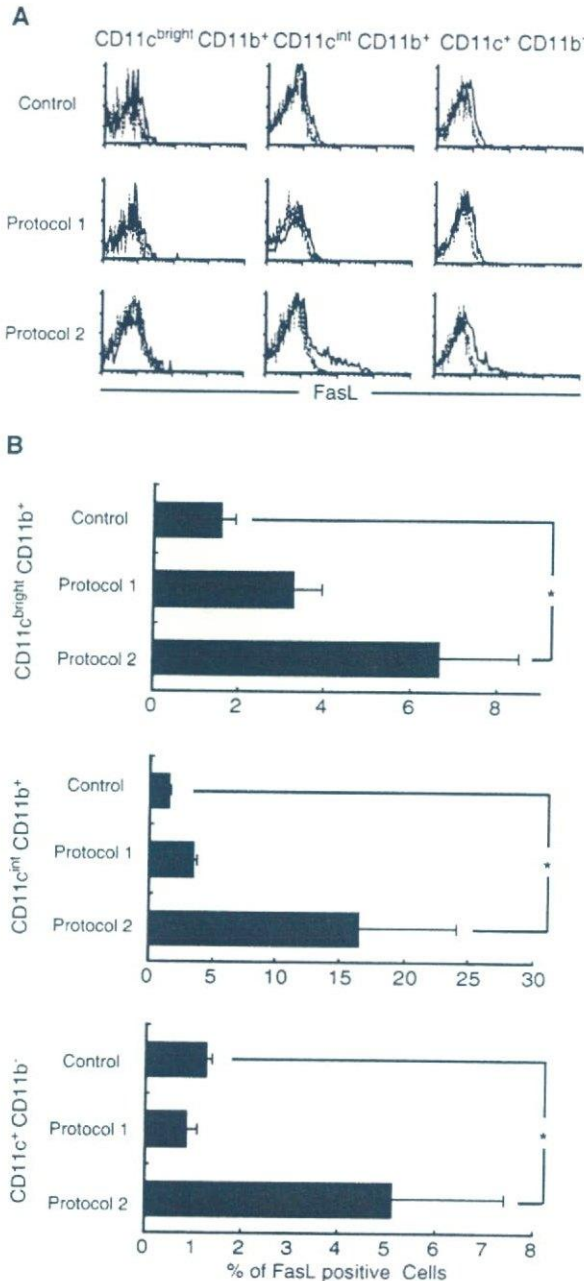


Fig. 4. Dendritic cells from LPS-treated mice with up-regulated FasL expression on their surface. The splenocytes from control or LPS-treated B6 mice were stained with anti-CD11b-FITC and anti-CD11c Bio+ APC-streptavidin, together with anti-FasL-PE. The expression of FasL on the different splenic DC subsets was analyzed by flow cytometry. (A) Representative histograms of FasL expression on CD11c^{bright} CD11b⁺, CD11c^{int} CD11b⁺ and CD11c⁺ CD11b⁻ DCs, which were electronically gated as shown in Fig. 3A. Dotted lines represent negative control staining with isotype-matched mAbs. The FCM profiles shown are representative of five independent experiments. (B) Data are expressed as the percentage of cells staining positive for FasL. Statistical analyses of surface expression of FasL were performed using ANOVA (* $p < 0.05$ vs. control). Data represent mean \pm S.E.M. of five mice per group.

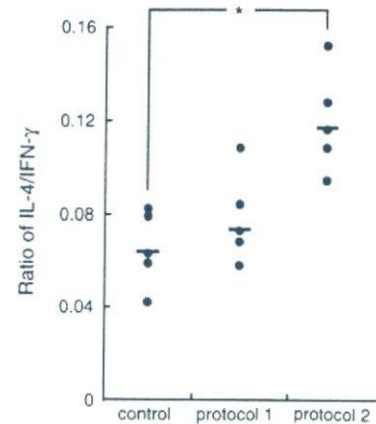


Fig. 5. Splenic APCs from endotoxin-tolerized mice induce Th 2-biased responses during the allogeneic MLR assay. The concentration of cytokines (pg/ml) in the MLR assay culture supernatants on day 5 was determined. The Th 1/Th 2 balance in each group was designated as the ratio of IL-4/IFN- γ . Each point represents an individual mouse. A single bar indicates the mean value for each group. Statistical analyses were performed using ANOVA (* $p < 0.05$ vs. control).

DCs subset that also expressed MHC class II and costimulatory molecules.

4.6. Splenic APCs from the endotoxin-tolerized mice induce Th 2-biased responses during the allogeneic MLR assay

Differences in the Th 1/Th 2-inducing function of DCs are considered to be the result of intrinsic differences between the distinct lineages of these cells. As compared to their CD11b⁺ myeloid counterparts, the CD11b⁻ lymphoid-related DCs have been shown, at least *in vitro*, to favor the development of Th 1-biased responses [19]. As shown in Fig. 3, the induction of ET caused the exclusive down-regulation of the expression of MHC class II and costimulatory molecules on CD11b⁻ lymphoid-related DCs. Such phenotypic alteration of the DCs may influence their Th 1/Th 2-driving capacity. To illustrate the Th 1/Th 2 balance, we determined the IL-4/IFN- γ ratio in the MLR assay supernatants. By using endotoxin-tolerized stimulators, a distinct shift in the Th 1/Th 2 balance toward the Th 2-type response was observed in the supernatant of the MLR assay culture (Fig. 5). Thus, the splenic APCs from the endotoxin-tolerized mice induced Th 2-biased responses during the allogeneic MLR assay.

5. Discussion

ET was initially described in animal models in which repetitive exposure to LPS was found to blunt LPS-associated mortality [3,4]. This mechanism may protect the host from developing a shock syndrome caused by the hyper-activation of monocytes or macrophages due to persistent LPS load. It has been recently demonstrated that ET induction also protects the host from ischemia/reperfusion injury in several organs [10,11], thus indicating the possibility of a novel approach involving the use of synthetic LPS analogs to prevent organ ischemia/reperfusion injury. In addition to these favorable effects, the impaired capacity of endotoxin-tolerized monocytes

to stimulate various T cell responses have also been demonstrated [7].

In the present study, the allogeneic MLR assays revealed that splenocytes from the endotoxin-tolerized mice completely inhibited the proliferation capacity of allogeneic CD4⁺ and CD8⁺ T cells. This result indicates that ET induction in transplant donors could impair direct antigen presentation, and this in turn might prevent the rejection reaction of the allografts. Consistent with this assumption, ET induction in donor animals prior to harvesting heart grafts resulted in prolonged graft survival in allogeneic recipients. It is likely that the antigen-presenting capacity of cardiac APCs was impaired by ET induction; a similar phenomenon occurs in splenic APCs. Alternatively, the prolonged survival of the endotoxin-tolerized heart allografts might be due to the migration of the DCs from the heart following LPS treatment. It has been previously reported that systemic administration of LPS leads to a reduction in the number of DCs in nonlymphoid tissues, including the tissues of the heart and kidney [20]. Further, DC migration from the heart following LPS treatment may increase the proportion of myeloid-related DCs in the splenocytes of endotoxin-tolerized mice; this was observed in this study. An alternative explanation might be that myocardiocytes build up a resistance to alloimmune-induced cytotoxicity through exposure to the endotoxin. Further studies are required to address these possibilities.

Since DCs in allogeneic organ grafts are thought to play a pivotal role in initiating T cell responses after transplantation and a key role in regulating these T cell responses, we determined the phenotypical alterations in the different lineages of splenic DCs. The 2 principal subsets identified in mouse liver, spleen and lymphoid tissue are referred to as the myeloid (CD11c⁺CD11b⁺) and lymphoid (CD11c⁺CD11b⁻)-related DC subsets [16,17]. These DCs are distinguished by their reciprocal expression of CD8 α and CD11b, and were initially thought to have a distinct lineage and functions. Cells within the CD11c⁺CD11b⁺ subset do not express CD8 α or DEC-205; however, they express F4-80, 33D-1 and other myeloid-related markers; this suggests their myeloid origin. ET induction led to an increase in the proportion of myeloid-related DCs expressing molecules necessary for antigen presentation, but reduced the proportion of lymphoid-related DCs expressing these molecules. It has been demonstrated that the myeloid-related DCs can induce large amounts of Th 2 cytokines, IL-4 and IL-10, in addition to IFN- γ and IL-2, whereas the lymphoid-related DCs can induce high levels of Th 1 cytokines, IFN- γ and IL-2, but little or no Th 2 cytokines [19]. Consistent with this fact and the alteration in the proportion of DC subsets among the endotoxin-tolerized splenocytes, the down-regulation of Th 1 cytokine production with a shift toward the Th 2 cytokine response was observed during the MLR assay that used the endotoxin-tolerized stimulators in the present study. Recent studies which demonstrated that ET correlates with the inhibition of NF- κ B translocation in DCs provided evidence that NF- κ B activation is responsible for DC maturation and activation [21,22]. Hence, it is likely that the disruption of NF- κ B activation may be a mechanism that contributes to the ET-mediated interference in DC expression of MHC class II and costimulatory molecules and cytokine secretion, which, in turn, diminishes the

alloimmune responses. Alternatively, the reduced expression levels of MHC class II molecules on lymphoid-related DCs in the endotoxin-tolerized splenocytes might be caused by the reduced expression level of the class II transactivator (CIITA) that regulates the expression of MHC class II molecules. This assumption was based on the results of a previous study, which demonstrated that reduced MHC class II expression in LPS-treated monocytic cells is a consequence of reduced CIITA expression [23]. Further, it has been reported that CIITA plays a key role in repressing Th 2-type cytokine expression since naive CD4⁺ T cells differentiate toward the Th 1 lineage [24]. Therefore, reduced CIITA expression in the endotoxin-tolerized stimulators might be responsible for the Th 2 polarization observed in the present study. Further studies are required to verify these possibilities.

In addition to the ET-mediated interference in the DC expression of MHC class II and costimulatory molecules and cytokine secretion, the enhanced expression of FasL on both myeloid- and lymphoid-related DCs might also be involved in the mechanisms for diminishing alloimmune responses (Fig. 4). It is well known that FasL engagement inhibits CD4⁺ T cell proliferation, cell-cycle progression and IL-2 secretion [18]. Considering that FasL and CD80 molecules on DCs play counter-regulatory roles in the proliferation and survival of T cells following DC–T cell interaction [25,26], we assume that the diminishing alloimmune responses are due to a comprehensive alteration in the expression of these molecules on the endotoxin-tolerized DCs.

We are the first to demonstrate that ET induction in donor animals inhibits alloimmune responses. Since the administration of LPS is not a conditioning treatment that would be considered plausible in human organ donors, the development of nontoxic analogs of LPS for therapeutic use might be required in order to apply this approach in clinical situations.

Acknowledgments

The authors thank Drs. Hidetaka Hara, Takashi Onoe, Wendy Zhou and Hiroshi Mitsuta for their advice.

This work was supported by a Grant-in-Aid for Scientific Research (B) and Exploratory Research from the Japan Society for the Promotion of Science and Grant-in-Aid for the Creation of Innovations through Business-Academic-Public Sector Cooperation, Ministry of Education, Culture, Sports, Science and Technology.

References

- [1] Rietschel ET, Kirikae T, Schade FU, Mamat U, Schmidt G, Loppnow H, et al. Bacterial endotoxin: molecular relationships of structure to activity and function. *FASEB J* 1994;8(2):217–25.
- [2] Ding AH, Nathan CF, Stuehr DJ. Release of reactive nitrogen intermediates and reactive oxygen intermediates from mouse peritoneal macrophages. Comparison of activating cytokines and evidence for independent production. *J Immunol* 1988;141(7):2407–12.
- [3] Brooke MS. Conversion of immunological paralysis to immunity by endotoxin. *Nature* 1965;206(984):635–6.
- [4] Greisman SE, Young EJ, Workman JB, Ollodart RM, Hornick RB. Mechanisms of endotoxin tolerance. The role of the spleen. *J Clin Invest* 1975;56(6):1597–607.

- [5] Chae BS. Comparative study of the endotoxemia and endotoxin tolerance on the production of Th cytokines and macrophage interleukin-6: differential regulation of indomethacin. *Arch Pharm Res* 2002;25(6):910–6.
- [6] Hirohashi N, Morrison DC. Low-dose lipopolysaccharide (LPS) pretreatment of mouse macrophages modulates LPS-dependent interleukin-6 production in vitro. *Infect Immun* 1996;64(3):1011–5.
- [7] Wolk K, Docke WD, von Baehr V, Volk HD, Sabat R. Impaired antigen presentation by human monocytes during endotoxin tolerance. *Blood* 2000;96(1):218–23.
- [8] Ziegler-Heitbrock HW. Molecular mechanism in tolerance to lipopolysaccharide. *J Inflamm* 1995;45(1):13–26.
- [9] Cohen N, Morisset J, Emilie D. Induction of tolerance by *Porphyromonas gingivalis* on APCs: a mechanism implicated in periodontal infection. *J Dent Res* 2004;83(5):429–33.
- [10] Heemann U, Szabo A, Hamar P, Muller V, Witzke O, Lutz J, et al. Lipopolysaccharide pretreatment protects from renal ischemia/reperfusion injury: possible connection to an interleukin-6-dependent pathway. *Am J Pathol* 2000;156(1):287–93.
- [11] Dominguez FE, Siemers F, Flohe S, Nau M, Schade FU. Effects of endotoxin tolerance on liver function after hepatic ischemia/reperfusion injury in the rat. *Crit Care Med* 2002;30(1):165–70.
- [12] Toyoda T, Kassell NF, Lee KS. Induction of tolerance against ischemia/reperfusion injury in the rat brain by preconditioning with the endotoxin analog diphosphoryl lipid A. *J Neurosurg* 2000;92(3):435–41.
- [13] Kiani A, Tschiersch A, Gaboriau E, Otto F, Seiz A, Knopf HP, et al. Downregulation of the proinflammatory cytokine response to endotoxin by pretreatment with the nontoxic lipid A analog SDZ MRL 953 in cancer patients. *Blood* 1997;90(4):1673–83.
- [14] Tanaka Y, Ohdan H, Onoe T, Asahara T. Multiparameter flow cytometric approach for simultaneous evaluation of proliferation and cytokine-secreting activity in T cells responding to allo-stimulation. *Immunol Invest* 2004;33(3):309–24.
- [15] Ohdan H, Yang YG, Shimizu A, Swenson KG, Sykes M. Mixed chimerism induced without lethal conditioning prevents T cell- and anti-Gal α 1,3 Gal-mediated graft rejection. *J Clin Invest* 1999;104(3):281–90.
- [16] Pulendran B, Lingappa J, Kennedy MK, Smith J, Teepe M, Rudensky A, et al. Developmental pathways of dendritic cells in vivo: distinct function, phenotype, and localization of dendritic cell subsets in FLT3 ligand-treated mice. *J Immunol* 1997;159(5):2222–31.
- [17] Maraskovsky E, Brasel K, Teepe M, Roux ER, Lyman SD, Shortman K, et al. Dramatic increase in the numbers of functionally mature dendritic cells in Flt3 ligand-treated mice: multiple dendritic cell subpopulations identified. *J Exp Med* 1996;184(5):1953–62.
- [18] Boshell M, McLeod J, Walker L, Hall N, Patel Y, Sansom D. Effects of antigen presentation on superantigen-induced apoptosis mediated by Fas/Fas ligand interactions in human T cells. *Immunology* 1996;87(4):586–92.
- [19] Pulendran B, Smith JL, Caspary G, Brasel K, Pettit D, Maraskovsky E, et al. Distinct dendritic cell subsets differentially regulate the class of immune response in vivo. *Proc Natl Acad Sci U S A* 1999;96(3):1036–41.
- [20] Roake JA, Rao AS, Morris PJ, Larsen CP, Hankins DF, Austyn JM. Dendritic cell loss from nonlymphoid tissues after systemic administration of lipopolysaccharide, tumor necrosis factor, and interleukin 1. *J Exp Med* 1995;181(6):2237–47.
- [21] Caldwell S, Heitger A, Shen W, Liu Y, Taylor B, Ladisch S. Mechanisms of ganglioside inhibition of APC function. *J Immunol* 2003;171(4):1676–83.
- [22] Neurath MF, Becker C, Barbuiescu K. Role of NF-kappaB in immune and inflammatory responses in the gut. *Gut* 1998;43(6):856–60.
- [23] Wolk K, Kunz S, Crompton NE, Volk HD, Sabat R. Multiple mechanisms of reduced major histocompatibility complex class II expression in endotoxin tolerance. *J Biol Chem* 2003;278(20):18030–6.
- [24] Patel DR, Kaplan MH, Chang CH. Altered Th1 cell differentiation programming by CIITA deficiency. *J Immunol* 2004;173(9):5501–8.
- [25] Lu L, Qian S, Hershberger PA, Rudert WA, Lynch DH, Thomson AW. Fas ligand (CD95L) and B7 expression on dendritic cells provide counter-regulatory signals for T cell survival and proliferation. *J Immunol* 1997;158(12):5676–84.
- [26] Kronin V, Vremec D, Winkel K, Classon BJ, Miller RG, Mak TW, et al. Are CD8⁺ dendritic cells (DC) veto cells? The role of CD8 on DC in DC development and in the regulation of CD4 and CD8 T cell responses. *Int Immunol* 1997;9(7):1061–4.

ORIGINAL ARTICLE

Safety of donor right hepatectomy for adult-to-adult living donor liver transplantation

Toshiyuki Itamoto, Kentaro Emoto, Hiroshi Mitsuta, Saburo Fukuda, Hideki Ohdan, Hirotaka Tashiro and Toshimasa Asahara

Department of Surgery, Division of Frontier Medical Science, Programs for Biomedical Research, Graduate School of Biomedical Science, Hiroshima University, Hiroshima, Japan

Keywords

CT cholangiography, donor hepatectomy, living donor liver transplantation, morbidity, volumetry.

Correspondence

Toshiyuki Itamoto, Department of Surgery, Division of Frontier Medical Science, Programs for Biomedical Research, Graduate School of Biomedical Science, Hiroshima University, Hiroshima, Japan. Tel.: +81 82 257 5222; fax: +81 82 257 5222; e-mail: titamoto@hiroshima-u.ac.jp

Received: 23 July 2005

Revision requested: 17 August 2005

Accepted: 8 December 2005

doi:10.1111/j.1432-2277.2006.00269.x

Summary

The purpose of this study was to ascertain the usefulness of preoperative evaluations of donors by computed tomography (CT) volumetry and CT cholangiography for prevention of unexpected liver failure and biliary complications after donor right hepatectomy for adult-to-adult living donor liver transplantation. Fifty-two donors who underwent right hepatectomy without the middle hepatic vein were enrolled in this study. The values of graft weight (GW) were significantly correlated with those of estimated graft volume (GV; $P < 0.0001$). GW was predicted by the following formula: $GW = 155.25 + 0.658 \times GV$; $r^2 = 0.489$. CT cholangiography revealed anatomical variants of biliary structure in one-third of the donors and also clearly showed one or two small biliary branches from the caudate lobe to the right hepatic ducts or the confluence in 58% of the donors. Biliary leakage, which was treated by conservative therapy, occurred in only one donor (1.9%). No donors received homologous blood transfusion. Hyperbilirubinemia (serum total bilirubin >5 mg/dl) occurred in 5.8% of the donors during their early postoperative periods. Precise evaluations of liver remnant volume by CT volumetry and biliary variation by CT cholangiography are essential for performing safe donor hepatectomy, preventing hepatic insufficiency and minimizing the risk of biliary tract complications.

Introduction

As the first successful living donor liver transplantation (LDLT) from an adult donor to an adult recipient [1], LDLT is rapidly emerging worldwide as an effective treatment for selected adult patients with end-stage liver disease [2,3]. The prevalence of adult-to-adult LDLT has led to application of a right lobe graft to the procedure for providing a sufficient hepatic mass. Despite impressive results of LDLT, there still is considerable debate concerning donor safety, especially in LDLT using a right lobe graft. Serious postoperative complications resulting from hepatic parenchymal loss occur more frequently in donors undergoing right hepatectomy than in those undergoing left hepatectomy or left lateral segmentectomy [3,4]. Loss of a large part of the liver resulted in hepatic insufficiency or death in sev-

eral donors [5,6,7]. Precise evaluations of donor liver by imaging modalities before surgery are important for preventing unexpected hepatic insufficiency in the donor.

Biliary complications such as bile leakage and biliary stricture are also frequent and sometimes serious in donors who have undergone right hepatectomy [3,8]. In LDLT using a right lobe graft, precise identification of right biliary duct variants in the donor before the operation is critical for the successfully and safely performing not only donor hepatectomy but also biliary reconstruction in the recipient. We present here results of our evaluations for donors in adult-to-adult LDLT, focusing on preoperative evaluation of liver volume by computed tomography (CT) and of biliary anatomy by CT cholangiography, and outcomes of donors who had undergone right hepatectomy.

Patients and methods

From June 1991 to May 2005, 64 donors underwent donor hepatectomy for adult-to-adult LDLT at Hiroshima University Hospital (Hiroshima, Japan) by a single team. Of them, 52 donors who underwent right hepatectomy without the middle hepatic vein were enrolled in this study. Forty-eight (92%) of the 52 donors had undergone donor hepatectomy in the past 4 years. The donors included 31 men and 21 women with a median age of 29 years (range: 18–61 years). The donors consisted of four parents, 32 children, nine siblings, six spouses and one uncle. Mean and median follow-up periods were 28 and 24 months respectively.

The median age of the recipients was 51 years (range: 20–69 years). Underlying liver diseases of transplant recipients were cirrhosis from hepatitis virus infection in 30 patients (22 with hepatocellular carcinoma), fulminant hepatic failure in seven patients, autoimmune hepatitis in four patients, primary biliary cirrhosis in four patients, alcoholic liver cirrhosis in three patients, retransplantation in two patients and metastatic liver tumors from insulinoma, Wilson disease each in one patient.

Data were obtained from medical record review and follow-up was complete as of 30 July 2005. Postoperative complication was defined as any event satisfying the criteria advocated by Broering *et al.* [9], who modified the classification of Clavian *et al.* [10] to adapt it to a living donor situation.

Donor selection and evaluation

All donors were evaluated before surgery by a hepatologist and psychologist. Acceptance criteria for living donors included age between 18 and 65 years; relation to the recipient within the third degree of consanguinity; negative results of serological tests for hepatitis B and C and human immunodeficiency viruses; adequate psychological support; normal hematologic, liver and renal functions; and normal electronic cardiogram. In terms of ABO blood group compatibility, we had accepted ABO-incompatible donors during our initial experiences. However, we later considered only ABO-identical or ABO-compatible donors to be acceptable as two recipients who received ABO-incompatible grafts died of acute rejection. Eligible donors preceded to imaging studies, including chest and abdominal radiography, abdominal ultrasonography and CT for exclusion of any unrecognized diseases. CT was also used for volumetric study, delineation of vascular anatomy, and evaluation of the degree of fat content. Measurement of graft volume by the method of Heymsfield *et al.* [11] and analysis of CT images has been replaced as case number 6 of our series

by a method using Advantage Workstation (version 3.1, GE Medical Systems, Milwaukee, WI, USA) and Zio 900 M (Zio software, Tokyo, Japan) [12].

When estimated liver remnant volume in the donor accounted for <30%, the candidate, in principle, was considered to be unsuitable as a living donor. If it was suspected from results of imaging studies that a potential donor suffered from fatty liver, liver biopsy was performed preoperatively and mild fatty liver (<10% of fat storage) was considered to be acceptable for donation. Other invasive procedures such as hepatic arteriography and endoscopic retrograde cholangiopancreatography were not performed in any donors. CT cholangiography was performed for the evaluation of biliary anatomy for all donors except the initial six cases [12]. The biliary anatomy in donors was classified into four types, based on the tributary from the posterior segment [13] (Fig. 2).

The type of hepatectomy was selected according to the following criteria: ratio of estimated graft volume (GV) to standard liver volume of the recipient exceeding 40% and/or ratio of estimated GV to body weight of the recipient exceeding 0.8%. Standard liver volume of the recipient was calculated according to the formula proposed by Urata *et al.* [14]. Four hundred milliliters of autologous blood was stored routinely before the operation except in the setting of emergent transplantation.

Donor surgical procedure

The abdomen was entered through an inverted L-shaped incision. After cholecystectomy with insertion of a 5-Fr catheter through the cystic duct stump for subsequent intraoperative cholangiography, intraoperative ultrasound was performed to confirm the anatomy of the hepatic vein and to decide the parenchymal transection plane, with special attention given to the sizes of tributaries draining into the middle hepatic vein from the anterior segment. The right hepatic lobe was fully mobilized, preserving the significant (>5 mm) short hepatic veins for later reconstruction. The right hepatic artery was dissected and exposed only to the right side of the common bile duct. Along the demarcation line emerging after transient occlusion of the right hepatic artery and right portal vein, the transection line was determined. Parenchymal transection was performed using an ultrasonic dissector (Sonop 5000; Aloka Co., Ltd., Tokyo, Japan). No inflow or outflow occlusion was applied during the parenchymal transection. After completion of parenchymal transection, intraoperative cholangiography was performed and the presumed point of bile duct division was marked with a stainless clip to confirm adequate residual length, which is 2–3 mm on the proximal side of the bile duct, and to avoid narrowing the common bile duct of the donor. The

biliary stump and the divided hilar plate were closed by continuous 6-0 absorbable surgical sutures. A drain was inserted into the right subphrenic cavity. No dye via the cystic duct catheter was injected for a leak test.

The graft was perfused *ex situ* through the portal vein, initially with cold lactated Ringer's solution and then with cold University of Wisconsin solution (Viaspan; Dupont, Wilmington, DE, USA). Graft weight (GW) was measured on the back table.

Postoperative management

Postoperatively, the donors were observed in the surgical recovery room. To prevent serious complications, including pulmonary embolism and portal vein thrombosis, donors as case number 9 of our series received continuous intravenous infusion of 5000 units of heparin sodium per day for 2 days after hepatectomy. Intermittent mechanical leg compression was performed during the operation and until first mobilization. Liver function tests were performed on postoperative days 1, 2, 3, 7 and 10. CT was performed between postoperative days 6–14 for detecting intra-abdominal or intrathoracic fluid collection or for evaluating regeneration of the liver remnant.

Statistical analysis

Data are presented as medians with ranges in parentheses. Continuous variables were compared using a two-tailed, unpaired *t*-test for independent samples. Categorical data were compared using the chi-square test. A *P*-value <0.05 was considered to be significant. Correlations between continuous data were identified by linear regression analysis. All statistical analyses were performed using the StatView 5.0 software package for Windows (SAS Institute Inc., Cary, NC, USA).

Results

Fifty-five potential donors were evaluated by our protocol, and three potential donors were considered to be unsuitable as donors because of unacceptable fatty liver, insufficient remnant liver volume <30% or asymptomatic cerebral aneurysm. There was no potential donor considered to be unsuitable as a donor by reason of having vascular or biliary tract variants.

Table 1 shows the demographics of the 52 donors and grafts. The median values of remnant liver volume, estimated GV, and estimated GV-to-standard liver volume ratio were 40.7%, 749 ml and 65.3% respectively. Remnant liver volumes in eight donors were <35% of their total liver volume. The median values of determined GW

Table 1. Donor and graft-related profiles.

No. of case	52
Gender	
Male	31
Female	21
Age (year)*	29 (18–61)
BMI (kg/m ²)*	21.4 (17.4–27.4)
Remnant liver volume (%)*	40.7 (28.9–51.9)
Remnant liver volume <35%	8/52 (15.4%)
Estimated GV (ml)*	749 (506–1221)
Estimated GV/SLV (%)*	65.3 (38.2–95.2)
GW (g)*	616 (478–1142)
GBWR (%)*	1.03 (0.67–2.31)

BMI, body mass index; GV, graft volume; SLV, standard liver volume; GW, graft weight; GBWR, graft-to-body weight ratio.

*Values are expressed as medians with ranges in parentheses.

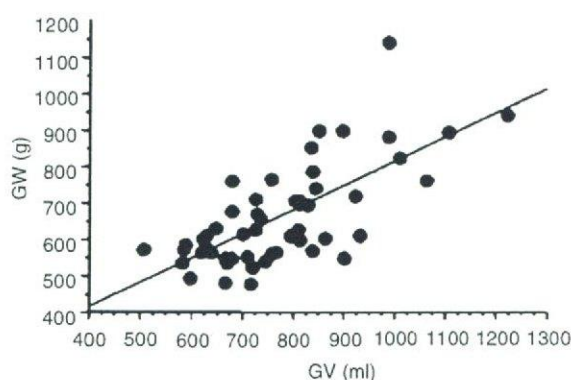


Figure 1 Regression analysis of the correlation between estimated graft volume (GV) by computed tomography and graft weight (GW) measured just after procurement in right lobe donors. The values of GW were significantly correlated with those of estimated GV ($P < 0.0001$). GW was predicted by the following formula: $GW = 155.25 + 0.658 \times GV$; $r^2 = 0.489$.

and GBWR were 616 g and 1.03% respectively. The estimated GV's exceeded the determined GW's in 44 (84.6%) of the 52 donors. The values of GW were significantly correlated with those of estimated GV ($P < 0.0001$). GW was predicted by the following formula: $GW = 155.25 + 0.658 \times GV$; $r^2 = 0.489$ (Fig. 1).

In 45 donors examined by CT cholangiography, type I bile duct was found in 34 donors (66.7%). Type II, type III and type IV bile ducts were found in 3 (6.7%), 4 (8.9%) and 7 (15.6%) donors respectively. One donor had a bile duct of a combination of types III and IV, and the bile duct in this donor was classified as to be type V (Fig. 2). CT cholangiography also revealed one or two small biliary branches from the caudate lobe to the right

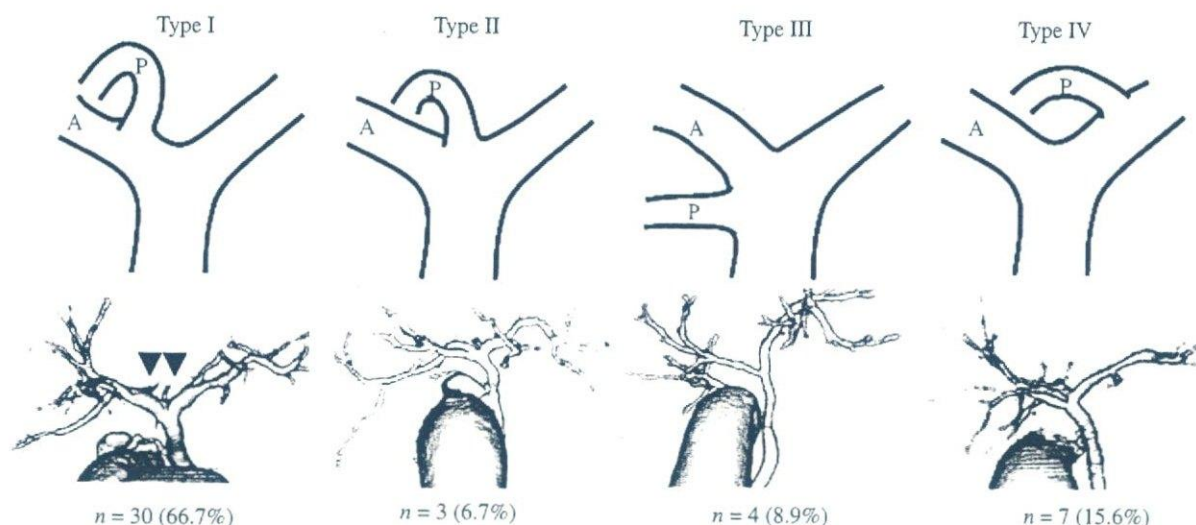


Figure 2 Biliary anatomy determined by CT cholangiography. Bile ducts in 45 donors were classified into four types based on the tributary from the posterior segment according to Nakamura's classification [13]. One donor had a bile duct of a combination of types III and IV. The figure was not shown. One-third of the donors had biliary tract variants. One or two small biliary branches from the caudate lobe to the right hepatic ducts or the confluence (arrowheads) were clearly detectable on images obtained by CT cholangiography.

hepatic ducts or the confluence in 26 (57.8%) of the 45 donors (Fig. 2).

Table 2 shows the outcomes of donor hepatectomy. The median operation time and blood loss were 415 min and 300 ml respectively. Ten (29.4%) of 34 donors whose autologous blood was preserved before the operation received autologous blood during or after the operation. No donors received homologous blood transfusion. How-

ever, one donor who suffered from postoperative bleeding followed by the formation of intra-abdominal hematoma received infusion of five units of fresh frozen plasma.

Five (9.6%) of the 52 donors had six postoperative complications, including peptic ulcer (grade II) in two donors, and bile leakage with necessity of endoscopic therapy (grade III), postoperative bleeding followed by the formation of hematoma with necessity of reoperation (grade III), pleural effusion (grade II) and keloid (grade I) each in one donor. No infectious complications such as wound infection occurred.

Changes in serum levels of total bilirubin and prothrombin time (INR) are shown in Fig. 3. Significant increases in serum total bilirubin occurred in all donors within 3 days after the operation. Three (5.8%) of the 52 donors suffered from hyperbilirubinemia (serum total bilirubin >5 mg/dl) during their early postoperative periods. However, the elevated total bilirubin level returned promptly to the preoperative value within 2 weeks after the operation in all donors (Fig. 3a). Similarly, INR that were significantly prolonged within several days after the operation returned promptly to the preoperative value within 1 week after the hepatectomies in all donors. In the case of postoperative bleeding, the values of INR were 2.20 and 2.19 on postoperative days 1 and 2 respectively (Fig. 3b). All 52 donors are alive and well for 1 month–13 years. Thirty-five of the 50 recipients are alive and 15 recipients died with a median follow-up period of 23 months.

Table 2. Operation-related data and postoperative results.

No. of case	52
Operation time (min)*	415 (320–785)
Blood loss (ml)*	300 (90–2400)
Use of preserved autologous blood (%)	10/34 (29.4)
Homologous blood transfusion	0/52 (0)
Postoperative complication (%)†	5/52 (9.3)
Intra-abdominal hematoma [n (grade‡)]	1 (III)
Bile leakage [n (grade‡)]	1 (III)
Pleural effusion [n (grade‡)]	1 (II)
Duodenal ulcer [n (grade‡)]	2 (II)
Keloid [n (grade‡)]	1 (I)
Reoperation rate (%)	1/52 (1.9)
Postoperative hospital stay (day)*	15 (11–24)
Re-admission rate (%)	2/52 (3.8)

*Values are expressed as medians with ranges in parentheses.

†A total of six complications occurred in five donors, resulting in an overall morbidity rate of 9.6%.

‡Postoperative complications were graded according to Broering's classification [9].

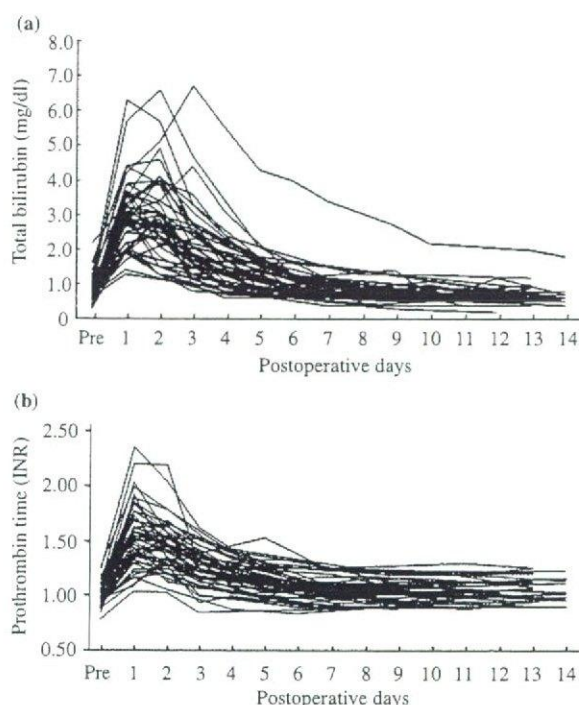


Figure 3 Changes in serum total bilirubin (a) and prothrombin time (INR) (b) before and after right hepatectomy in the 52 donors.

Discussion

Although mortality rate for donors undergoing hepatectomy has been reported to be <0.5% [2,5,8,15], the rate is far higher than that for kidney donation, which has a mortality rate of 0.03% [16]. One report claims that the mortality rate of right lobe donors is probably >1% [17]. However, the exact risk of death for donors remains uncertain because there is no worldwide registry of donor outcomes.

Precise preoperative evaluation of a donor is critical for performing LDLT successfully and safely in both the recipient and donor. Techniques and imaging modalities by which a donor liver have been estimated routinely in our adult-to-adult LDLT program include abdominal ultrasonography, CT with volumetry and CT cholangiography. Except for liver biopsy, which is mandatory for donors with fatty liver, invasive examinations such as hepatic arteriography and endoscopic retrograde cholangiopancreatography have not been performed. CT volumetry is an essential evaluation technique for both the donor and recipient. It has been reported that donor hepatectomies that exceed 70% of total liver volume led to hepatic insufficiency or death and that liver remnant volume should be kept to >30% of total liver volume [6,18]. By adhering to this policy and by precisely estimating the liver remnant volume in our program, there have been

no donors in whom hepatic insufficiency occurred after hepatectomies. Several authors have reported that the incidence of hyperbilirubinemia (total bilirubin >5 mg/dl) in donors who underwent right hepatectomy ranged from 3.7% to 18.7% [3,19,20]. In the present study, hyperbilirubinemia (total bilirubin >5.0 mg/dl) occurred in three donors (5.8%) between the first and third postoperative days. None of the eight donors whose remnant liver volume was <35% suffered from postoperative hyperbilirubinemia. It is thought that the infrequent postoperative hyperbilirubinemia in our program was a result of our precise volumetric evaluation for a potential donor, our strict policy for fatty liver and small blood loss during hepatectomies.

Graft-to-body weight ratio has been used when assessing the graft size of a potential donor to be suitable for the recipient and values <0.8% have been associated with increased post-transplantation mortality [21]. As shown in the present study, estimated GV tended to be overestimated compared with GW determined after graft procurement as reported previously [22], whereas estimated GV significantly correlated with GW. The main cause of the overestimation may be related to the difference between the vital liver filled with blood *in vivo* and the graft that is in a state of collapse *ex vivo*. Moreover, since the kind of imaging modality used, the performance, and the method by which GV is measured are different in transplant programs, it is necessary to correct the error using a conversion formula calculated in each transplant program.

A systematic review has shown that reported donor morbidity rates in leading LDLT programs worldwide range from 0% to 67% and has indicated that the differences are likely to be caused by varying definitions of complications [23]. Recently, a new and strict classification of postoperative complications for donor hepatectomy has been advocated to resolve the confusion [9]. Morbidity in the present study according to the strict definition was only 9.6%, and biliary complication occurred in only one donor (1.9%). Complications in donors were more frequent in a center in which small-volume LDLT is performed [5]. In spite of our initial 52 experiences, the results are superior to those in other large series.

Biliary tract complications, including bile leakage and bile duct stricture, are the most frequent cause of morbidity in donor hepatectomy. Recent study showed that postoperative biliary complications occurred in 7–10% of donors who had undergone right hepatectomy [3,8,23]. Postoperative bile leakage can occur in the parenchymal transection surface of the liver, the repair site of the hepatic duct, and the caudate branches in the hilar plate [24]. However, bile leakage from the parenchymal transection surface of the liver rarely occurs in donor hepatectomies because the biliary ducts are not exposed on

the parenchymal transection surface as long as the parenchyma is transected along Cantlie's line. In the setting of hepatectomies except for donor hepatectomy, Lo *et al.* [25] reported that left-sided major hepatectomy was an independent risk factor for the development of postoperative bile leakage because of the risk of damaging the right posterior segment bile duct draining into the left duct. However, in donor hepatectomies, precise preoperative assessments of biliary variants using CT cholangiography make it possible to prevent this type of biliary injury. Actually, this type of variant was confirmed preoperatively by CT cholangiography in 15.6% of our donors, and no biliary injury occurred in these donors. Accordingly, in donor hepatectomies, postoperative bile leakage from caudate branches at the hilar plate is thought to be dominant, because the hepatic ducts are sharply transected very close to the confluence. CT cholangiography enabled us to identify clearly not only various types of biliary tract variant but also small biliary branches from the caudate lobe to the right hepatic ducts or the confluence in the majority of donors. Moreover, preoperative CT cholangiography combined with intraoperative cholangiography has enabled us to divide the right hepatic duct at a suitable portion. Consequently, preoperative CT cholangiography and intraoperative cholangiography resulted in a low biliary complication rate (1.9%) in our program.

Another fatal and serious complication in donors is pulmonary embolism caused by deep vein thrombosis, which can occur following any kind of operation. There has been controversial as to whether it is necessary to administer heparin to a donor during the perioperative period, though prophylactic treatment such as intermittent mechanical leg compression in a donor during the operation and until first mobilization is mandatory. In donor hepatectomy, coagulation abnormalities observed immediately after surgery may be related mostly to blood loss and to the diluting effect of intraoperative infused fluids, although the extent of resection appears to be the most important factor in the extension of the prothrombin time observed until the first postoperative day [26]. The present study showed that significant prolongation of prothrombin time occurred on the first postoperative day and values of INR > 2.0 were observed in 3 donors, although the abnormal values returned to preoperative values within 1 week after the operation. Actually, one donor sustained intra-abdominal bleeding on the first postoperative day, which was not massive but significant, and INR at that time was 2.2. Hemostasis was obtained by discontinuance of heparin administration and by administration of 400 ml banked fresh frozen plasma and 400 ml stored autologous blood. It is necessary to pay special attention to administration of heparin for donors undergoing right hepatectomy.

In conclusion, precise evaluations of liver remnant volume by CT volumetry and biliary variation at the hilum by CT cholangiography are mandatory for performing safe right hepatectomy in a donor, preventing not only serious complications such as hepatic insufficiency but also biliary tract complications. Further efforts should be put into the technical refinements in donor hepatectomy, perioperative management, and precise preoperative evaluation for donor candidates with the goal of achieving a zero complication rate. Moreover, the long-term adverse effect of loss of as much as 60% of the donor's liver on the donor's health remains unknown, and transplant centers should continue their follow-up.

References

1. Hashikura Y, Makuuchi M, Kawasaki S, *et al.* Successful living-related partial liver transplantation to an adult patient. *Lancet* 1994; **343**: 1233.
2. Trotter JF, Wachs M, Everson GT, Kam I. Adult-to-adult transplantation of the right hepatic lobe from a living donor. *N Engl J Med* 2002; **346**: 1074.
3. Lo CM. Complications and long-term outcome of living liver donors: a survey of 1508 cases in five Asian centers. *Transplantation* 2003; **75**: S12.
4. Fujita S, Kim II, Uryuhara K, *et al.* Hepatic grafts from live donors: donor morbidity for 470 cases of live donation. *Transpl Int* 2000; **13**: 333.
5. Brown RS Jr, Russo MW, Lai M, *et al.* A survey of liver transplantation from living adult donors in the United States. *N Engl J Med* 2003; **348**: 818.
6. Akabayashi A, Slingsby BT, Fujita M. The first donor death after living-related liver transplantation in Japan. *Transplantation* 2004; **77**: 634.
7. Broering DC, Sterneck M, Rogiers X. Living donor liver transplantation. *J Hepatol* 2003; **38**: S119.
8. Umeshita K, Fujiwara K, Kiyosawa K, *et al.* Operative morbidity of living liver donors in Japan. *Lancet* 2003; **362**: 687.
9. Broering DC, Wilms C, Bok P, *et al.* Evolution of donor morbidity in living related liver transplantation: a single-center analysis of 165 cases. *Ann Surg* 2004; **240**: 1013.
10. Clavien PA, Camargo CA, Croxford R, Langer B, Levy GA, Greig PD. Definition and classification of negative outcomes in solid organ transplantation. Application in liver transplantation. *Ann Surg* 1994; **220**: 109.
11. Heymsfield SB, Fulenwider T, Nordlinger B, Barlow R, Sones P, Kutner M. Accurate measurement of liver, kidney, and spleen volume and mass by computerized axial tomography. *Ann Intern Med* 1979; **90**: 185.
12. Ishifuro M, Horiguchi J, Nakashige A, *et al.* Use of multi-detector row CT with volume renderings in right lobe living liver transplantation. *Eur Radiol* 2002; **12**: 2477.
13. Nakamura T, Tanaka K, Kiuchi T, *et al.* Anatomical variations and surgical strategies in right lobe living donor liver

- transplantation: lessons from 120 cases. *Transplantation* 2002; **73**: 1896.
14. Urata K, Kawasaki S, Matsunami H, *et al.* Calculation of child and adult standard liver volume for liver transplantation. *Hepatology* 1995; **21**: 1217.
 15. Adam R, Lucidi V, Karam V. Liver transplantation in Europe: is there a room for improvement? *J Hepatol* 2005; **42**: 33.
 16. Johnson EM, Najarian JS, Matas AJ. Living kidney donation: donor risks and quality of life. *Clin Transplant* 1997; **231**.
 17. Surman OS. The ethics of partial-liver donation. *N Engl J Med* 2002; **346**: 1038.
 18. Fan ST, Lo CM, Liu CL, Yong BH, Chan JK, Ng IO. Safety of donors in live donor liver transplantation using right lobe grafts. *Arch Surg* 2000; **135**: 336.
 19. Choi SJ, Gwak MS, Kim MH, *et al.* Differences of perioperative liver function, transfusion, and complications according to the type of hepatectomy in living donors. *Transpl Int* 2005; **18**: 548.
 20. Yokoi H, Isaji S, Yamagiwa K, *et al.* Donor outcome and liver regeneration after right-lobe graft donation. *Transpl Int* 2005; **18**: 915.
 21. Kiuchi T, Kasahara M, Uryuhara K, *et al.* Impact of graft size mismatching on graft prognosis in liver transplantation from living donor. *Transplantation* 1999; **67**: 321.
 22. Fulcher AS, Szucs RA, Bassignani MJ, Marcos A. Right lobe living donor liver: preoperative evaluation of the donor with MR imaging. *AJR* 2001; **176**: 1483.
 23. Beavers KL, Sandler RS, Shrestha R. Donor morbidity associated with right lobectomy for living donor liver transplantation to adult recipients: a systematic review. *Liver Transpl* 2002; **8**: 110.
 24. Liu CL, Fan ST, Lo CM, Chan SC, Yong BH, Wong J. Safety of donor right hepatectomy without abdominal drainage: a prospective evaluation in 100 consecutive liver donors. *Liver Transpl* 2005; **11**: 314.
 25. Lo CM, Fan ST, Liu CL, Lai EC, Wong J. Biliary complication after hepatic resection. *Arch Surg* 1998; **133**: 156.
 26. Siniscalchi A, Begliomini B, Pietri LD *et al.* Increased prothrombin time and platelet counts in living donor right hepatectomy: implications for epidural anesthesia. *Liver Transpl* 2004; **10**: 1144.

Liver Sinusoidal Endothelial Cells That Endocytose Allogeneic Cells Suppress T Cells with Indirect Allospecificity¹

Daisuke Tokita,^{2*} Masayuki Shishida,^{2*} Hideki Ohdan,^{3*} Takashi Onoe,^{*} Hidetaka Hara,^{*} Yuka Tanaka,^{*} Kohei Ishiyama,^{*} Hiroshi Mitsuta,^{*} Kentaro Ide,^{*} Koji Arihiro,[†] and Toshimasa Asahara^{*}

A portal venous injection of allogeneic donor cells is known to prolong the survival of subsequently transplanted allografts. In this study, we investigated the role of liver sinusoidal endothelial cells (LSECs) in immunosuppressive effects induced by a portal injection of allogeneic cells on T cells with indirect allospecificity. To eliminate the direct CD4⁺ T cell response, C57BL/6 (B6) MHC class II-deficient *C2a^{tm1Ccum}* (C2D) mice were used as donors. After portal injection of irradiated B6 C2D splenocytes into BALB/c mice, the host LSECs that endocytosed the irradiated allogeneic splenocytes showed enhanced expression of MHC class II molecules, CD80, and Fas ligand (FasL). Due to transmigration across the LSECs from BALB/c mice treated with a portal injection of B6 C2D splenocytes, the naive BALB/c CD4⁺ T cells lost their responsiveness to stimulus of BALB/c splenic APCs that endocytose donor-type B6 C2D alloantigens, while maintaining a normal response to stimulus of BALB/c splenic APCs that endocytose third-party C3H alloantigens. Similar results were not observed for naive BALB/c CD4⁺ T cells that transmigrated across the LSECs from BALB/c FasL-deficient mice treated with a portal injection of B6 C2D splenocytes. Adaptive transfer of BALB/c LSECs that had endocytosed B6 C2D splenocytes into BALB/c mice via the portal vein prolonged the survival of subsequently transplanted B6 C2D hearts; however, a similar effect was not observed for BALB/c FasL-deficient LSECs. These findings indicate that LSECs that had endocytosed allogeneic splenocytes have immunosuppressive effects on T cells with indirect allospecificity, at least partially via the Fas/FasL pathway. *The Journal of Immunology*, 2006, 177: 3615–3624.

It has been postulated that the liver might be a site for the induction of tolerance to exogenous MHC class II-restricted Ags that enter the organ in large numbers via portal circulation from the gut (1, 2). This phenomenon has been applied as a strategy to achieve the ultimate goal in transplantation; the induction of tolerance in T cells with allospecificity, i.e., single treatment with a portal venous injection of allogeneic cells succeeds in inducing persistent donor-specific tolerance across multiple minor histocompatibility and MHC class I incompatible barriers (3, 4). Such tolerance could be induced by injecting not only living allogeneic cells but also soluble Ags (5, 6), thereby increasing the possibility of efficiently inducing tolerance in T cells with indirect allospecificity. In addition to portal injection of donor cells, other treatments such as the administration of immunosuppressants (7–10) and costimulatory blockades (11) are usually required to induce donor-specific tolerance across MHC class II incompatible barriers. This suggests that the tolerizing effects of portal injection

of donor cells might be more efficient in T cells with indirect allospecificity than in T cells with direct allospecificity.

Portal injection-induced tolerance in T cells with indirect allospecificity might be a consequence of presentation of allopeptides by the host APCs in the liver to these T cells. The ability to present exogenous Ags on MHC class I or II molecules is restricted to Kupffer cells and dendritic cells in the liver. In portal injection-induced tolerance, the importance of Ag presentation by Kupffer cells is emphasized by the prevention of Ag sequestration and tolerance following the administration of gadolinium chloride (a rare earth metal that prevents Kupffer cell phagocytosis) (12, 13). Liver dendritic cells possess unique Ag-presenting properties and exhibit low expression of costimulatory molecules. Furthermore, the liver dendritic cells preferentially induce Th2 responses, suggesting that these cells mediate tolerogenicity (14, 15). In addition to Kupffer cells and liver dendritic cells, liver sinusoidal endothelial cells (LSECs),⁴ which line the hepatic sinusoids, are also capable of presenting soluble exogenous Ags to T cells that possess transgenic TCRs (16–18). Although a number of studies have demonstrated the importance of Ag presentation by Kupffer cells and liver dendritic cells in portal injection-induced transplantation tolerance, the role of Ag presentation by LSECs in such immune tolerance has not been investigated. In this study, we demonstrated that LSECs actively endocytose allogeneic splenocytes injected via the portal vein and that CD4⁺ T cells with indirect allospecificity lose their responsiveness on contact with such LSECs, at least partially via the Fas/Fas ligand (FasL) pathway. This study is the first to demonstrate that LSECs are capable of

*Department of Surgery, Division of Frontier Medical Science, Programs for Biomedical Research, Graduate School of Biomedical Sciences, Hiroshima University, Hiroshima, Japan; and †Department of Anatomical Pathology, Hiroshima University Hospital, Hiroshima, Japan

Received for publication December 23, 2004. Accepted for publication June 28, 2006.

The costs of publication of this article were defrayed in part by the payment of page charges. This article must therefore be hereby marked advertisement in accordance with 18 U.S.C. Section 1734 solely to indicate this fact.

¹ This study was supported in part by a Grant-in-Aid for Exploratory Research (no. 17659389) of the Ministry of Education, Culture, Science and Technology from the Japan Society for the Promotion Science.

² D.T. and M.S. contributed equally to this work and should be considered as first authors.

³ Address correspondence and reprint requests to Dr. Hideki Ohdan, Department of Surgery, Division of Frontier Medical Science, Programs for Biomedical Research, Graduate School of Biomedical Sciences, Hiroshima University, 1-2-3 Kasumi, Minami-Ku, Hiroshima 734-8551, Japan. E-mail address: ohdan@hiroshima-u.ac.jp

⁴ Abbreviations used in this paper: LSEC, liver sinusoidal endothelial cell; FasL, Fas ligand; Ac-LDL, acetylated low-density lipoprotein; FCM, flow cytometry; WT, wild type; MHLR, mixed hepatic constituent cell-lymphocyte reaction; ILT, Ig-like transcript.

regulating a polyclonal population of nontransgenic T cells with certain specificity via the indirect pathway.

Materials and Methods

Mice

BALB/c (H-2^d), C57BL/6 (B6) (H-2^b), and C3H/HeN (C3H) (H-2^k) mice (8- to 12-wk-old females) were purchased from Clea Japan. B6 MHC class II-deficient (C2D) (B6.129S2-C2ta^{m1/Ccrmt}) mice and BALB/c-FasL^{gld} (BALB/c-gld) (CpT.C3-Tnfsf6^{gld}) mice were purchased from The Jackson Laboratory. All animals were maintained in a specific pathogen-free microisolator environment. Animal experiments were approved by the Institutional Review Board at Hiroshima University and were conducted in accordance with the guidelines of the National Institutes of Health (National Institutes of Health publication no. 86-23, revised 1985).

Portal venous injection of donor-type splenocytes

Splenocytes were prepared as a single-cell suspension after lyses of erythrocytes using an ammonium chloride/potassium solution. The splenocytes were irradiated (30 Gy) before treatment with a portal venous injection to eliminate possible graft-vs-host responses. Allogeneic splenocytes (30×10^6) in 0.5 ml of medium 199 (Sigma-Aldrich) containing 1% HEPES buffer were injected through the superior mesenteric vein using a 30-gauge needle.

Heterotopic heart transplantation

Donor-type heart allografts were transplanted. Cervical heterotopic heart transplantation was performed using the cuff technique modified from a previously described method (19). Briefly, the recipients were prepared before donor heart harvest to minimize the graft ischemic time. The right external jugular vein and the right common carotid artery were dissected free, mobilized as far as possible, and fixed to the appropriate cuffs. The cuffs were composed of polyethylene tubes (2.5F; Portex), the diameters of which were adjusted by physical extension. For anastomoses, the aorta and the main pulmonary artery of the harvested donor heart were drawn over the end of the common carotid artery and the external jugular vein, respectively. The graft ischemic time for the transplanted hearts was <30 min. The function of the grafts was monitored by daily inspection and palpation. Rejection was determined by the cessation of beating of the graft and was confirmed by histology.

Flow cytometry (FCM) analysis of anti-donor Abs

Indirect immunofluorescence staining of thymocytes from B6 mice was used to detect anti-donor-specific Abs. Cells (1×10^6) were incubated with 10 μ l of serially diluted mouse serum, washed, and incubated with FITC-conjugated rat anti-mouse IgM and IgG mAb (BD Pharmingen), then were subjected to FCM analysis.

Isolation of LSECs

It has been reported that elevated levels of CD105 expression are selectively detected on the microvascular and vascular endothelial cells in regenerating tissue undergoing active angiogenesis (20-22). Similarly, LSECs that have an exceptional capacity for angiogenesis express CD105 in higher quantities than the endothelia of the central veins or other vessels in the liver (23). Therefore, CD105⁺ cells were positively selected for the isolation of LSECs from the nonparenchymal cell fraction of the liver as follows. Disaggregated liver cells were obtained from untreated BALB/c mice or BALB/c mice that had been treated with portal injection by the two-step collagenase perfusion method (24, 25) and were centrifuged at $50 \times g$ for 1 min. The supernatant was centrifuged at $150 \times g$ for 5 min. The pellet was resuspended, and the total cells obtained were stained with biotin-conjugated anti-CD105 (MJ7/18) (eBioscience). Subsequently, the cells were counterstained with streptavidin microbeads (Miltenyi Biotec) and magnetically sorted using an autoMACS cell sorter (Miltenyi Biotec). This sorting technique yielded $2-7 \times 10^6$ cells/body in the positive fraction. To analyze the purity of LSECs, aliquots of the sorted fractions were cultured in the presence of acetylated low-density lipoprotein (Ac-LDL)-BODIPY (final concentration, 15 mg/ml) (Molecular Probes) in a DMEM culture medium containing 10% heat-inactivated FBS, 5 mM 2-ME, 1% HEPES buffer, 100 IU/ml penicillin, and 100 mg/ml streptomycin on collagen I-coated 35-mm tissue culture dishes (BD Biosciences Labware). This fluorescence-labeled lipoprotein is exclusively taken up by endothelial cells such as LSECs. After 12 h, the cells were stained with anti-CD11b PE (M1/70) to detect the expression of CD11b as a marker for Kupffer cells. The sorted CD105⁺ cells were stained with anti-CD45 FITC (30F11.1) to

detect the expression of CD45 as a marker for hemopoietic cells. These were purchased from BD Pharmingen.

Detection of LSECs that endocytose allogeneic splenocytes

B6 C2D splenocytes were washed in PBS and labeled with PKH26 (Sigma-Aldrich) for the detection of LSEC endocytosis. PKH26 labeling (2×10^{-6} M dye) was performed according to the manufacturer's protocol. Following the portal injection of the irradiated B6 C2D splenocytes (30×10^6 cells) labeled with PKH26 into BALB/c mice, the host LSECs were isolated as described earlier. Fc γ R-blocking Abs (rat anti-mouse CD16/32 mAb) (2.4G2) were used, followed by staining with anti-mouse I-A/I-E FITC (2G9), anti-CD40 FITC (HM40-3), anti-CD80 FITC (16-10A1), anti-CD86 FITC (GL1) (BD Pharmingen), or unlabeled anti-mouse CD95 Ligand (MFL3) (eBioscience). The unlabeled mAb was visualized using anti-Armenian hamster IgG FITC (H+L) (eBioscience). The cells were analyzed by FCM analysis gating on the CD105⁺ population. The LSECs that endocytosed the injected splenocytes were identified as PKH26-labeled cells by FCM analysis. FCM was performed using a FACSCalibur (BD Biosciences). LSECs were also observed under a relief contrast confocal microscope.

Transendothelial migration assay

The isolated LSECs obtained from the experimental animals were applied onto a fibronectin-coated (50 μ g/ml; Sigma-Aldrich) polycarbonate filter (pore size, 8 μ m; Costar) containing a cell culture insert (1×10^5 cells/well in a 48-well plate). After 12 h of culture, nonadherent cells were removed from the filter membrane by washing. For the analysis of cell proliferation in indirect MLR, splenocytes were labeled with 5 μ M CFSE (Molecular Probes) as described previously (26). CFSE-labeled syngeneic nonadherent splenocytes (10×10^6 cells/well) were overlaid on the monolayer of LSECs in the culture insert and incubated for 12 h. Splenocytes transmigration to the bottom of the individual wells were harvested. These cells were used as responder cells for the subsequent indirect MLR (see Fig. 4A).

Preparation of stimulator cells for indirect MLR

Donor-type B6 C2D or third-party C3H splenocytes (20×10^6 cells) were injected i.v. into BALB/c mice. Seven days after the injection, splenocytes were obtained from the BALB/c mice. These splenocytes were plated on 100-mm tissue culture dishes (Falcon 3003; BD Biosciences Labware). After incubation for 2 h, adherent cells were prepared as Ag-presenting stimulator cells for subsequent indirect MLR.

Indirect MLR assay

The Ag-presenting stimulator cells were irradiated with a dose of 30 Gy. CFSE-labeled responder cells were cultured with stimulator cells (in the ratio of 5:1) in a total volume of 2 ml of medium in a 24-well flat-bottom plate (BD Biosciences Labware) at 37°C in 5% CO₂ in the dark for 5 days.

Quantification of T cell proliferation

In the indirect MLR using CFSE-labeled lymphocytes, proliferating T cells were detected by a multiparameter FCM analysis as described previously (27, 28). The harvested cells were stained with anti-mouse CD4 PE mAb (GK1.5) (BD Pharmingen). Alloreactivities of the responder T cells were quantified based on their CFSE-fluorescence intensities. In CFSE-fluorescence histograms, CD4⁺ T cells were selected by gating and were subsequently analyzed for CFSE fluorescence. Dead cells were excluded from the analysis by light scatter and/or by using propidium iodide. Theoretically, the CFSE-fluorescence intensity of cells that have undergone one cell division is half the value of the CFSE-fluorescence intensity of undivided cells. According to this theory, the number of divisions of alloreactive T cells could be mathematically determined by the logarithmic CFSE intensities on the basis of the peak at the extreme right (the peak of undivided cells). The limit of detection is seven or eight division cycles caused by the compression of peaks as the CFSE intensity approaches autofluorescent levels. Thus, divisions beyond six cycles are indistinguishable and are collectively referred to as division 7+. A single-cell dividing n times will generate 2^n daughter cells. Using this mathematical relationship, the number of division precursors was extrapolated from the number of daughter cells of each division, and the number of times that mitotic events occurred in a CD4⁺ T cell subset was calculated. Using these values, mitotic indexes were calculated by dividing the total number of mitotic events by total precursors. Stimulation indexes were calculated by dividing the mitotic indexes of T cells responding to the splenic APCs pulsed with allogeneic cells by those of T cells responding to the control nonpulsed splenic APCs.

Intracellular cytokine staining for multiparameter FCM

Cytokine-secreting activity of T cells responding to allostimulation was determined as described previously (28). Following the indirect MLR culture, the cells were stimulated with 1 μ M ionomycin (Sigma-Aldrich), 10 ng/ml PMA (Sigma-Aldrich), and GolgiPlug (a protein transport inhibitor containing brefeldin A) (BD Pharmingen) (2 μ l in 2 ml of medium) for 4 h to enhance intracellular cytokine content without affecting cell proliferation, as described previously (29–32). After harvesting, the cultured cells were stained with PerCP-CyChrome (PerCP-Cy5.5)-conjugated anti-CD4 (GK1.5) (BD Pharmingen). Nonspecific Fc γ R binding of labeled Abs was blocked by CD16/32 (2.4G2) (BD Pharmingen). Furthermore, the cells were stained with annexin V (BD Pharmingen) for gating out dead or apoptotic cells. Following cell surface Ag and annexin V staining, the cells were fixed and permeabilized using Cytofix/Cytoperm solution (containing 4% paraformaldehyde and saponin) (BD Pharmingen) and Perm/Wash buffer (containing FBS and saponin) (BD Pharmingen) according to the manufacturer's instructions. For intracellular cytokine staining, PE-conjugated anti-IL-2 (JES6-1A12) and/or rat IgG1 (an isotype-matched control) were used.

Skin transplant model

Full-thickness tail skin was harvested from donor (B6 C2D) mice and grafted (2 pieces of ~0.5 cm in size) onto the dorsal side of recipient (BALB/c) mice. Rejection was defined as the complete necrosis of the skin grafts. Skin grafts were completely rejected on a regular basis within 14 days after transplantation. Splenocytes from mice sensitized with skin allografts after rejection were labeled with CFSE. CFSE-labeled nonadherent splenocytes were used as sensitized responder cells for the subsequent indirect MLR.

Intraportal adaptive transfer of LSECs

LSECs from BALB/c mice that were either untreated or treated with a portal injection of irradiated B6 C2D splenocytes (30×10^6 cells/mouse) were isolated after 12 h of the injection as described earlier. These LSECs were prepared as a single-cell suspension. The LSECs (2×10^6 cells) in 0.5 ml of medium 199 containing 1% HEPES buffer were injected through the superior mesenteric vein by using a 30-gauge needle.

Statistical analysis

The results were statistically analyzed using the log-rank test or *F* test and Student's *t* test of means, where appropriate. A *p* value of <0.05 was considered to be statistically significant.

Results

Portal venous injection of irradiated allogeneic splenocytes significantly prolonged the survival of subsequently grafted allogeneic hearts

To determine whether a portal venous injection of allogeneic cells could produce tolerance or hyporesponsiveness to allogeneic organ grafts, irradiated (30 Gy) splenocytes of either B6 MHC class II-deficient (C2D) or wild-type (WT) B6 mice were injected into BALB/c mice (30×10^6 cells/mouse) via the portal vein. Donor-type heart allografts were transplanted 7 days later. Survival curves of the grafted hearts are shown in Fig. 1. All untreated BALB/c mice rejected WT B6 hearts within 7–9 days and C2D B6 hearts within 8–10 days ($n = 5$ and 4, respectively). However, a portal injection of WT B6 splenocytes induced indefinite WT B6 heart allograft survival in 60% of BALB/c mice ($n = 5$). A portal injection of C2D B6 splenocytes induced indefinite C2D B6 heart allograft survival in 80% of BALB/c mice ($n = 5$). Thus, the portal injection of the irradiated allogeneic splenocytes effectively led to an indefinite acceptance of subsequently transplanted donor-type heart allografts, particularly in the absence and even in the presence of donor MHC class II molecules. To determine whether the acceptance of heart allografts was due to tolerization of cells responding to alloantigens, the Ab levels against B6 alloantigens were determined in the sera of the BALB/c recipients. The serum levels of anti-B6 IgG Ab gradually elevated and reached a plateau several weeks after the cardiac allograft transplantation in the BALB/c mice that had received the portal injection of irradiated

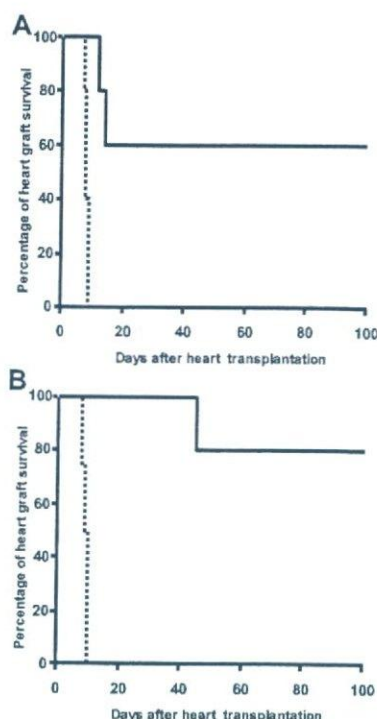


FIGURE 1. A portal venous injection of the irradiated allogeneic splenocytes leads to the indefinite acceptance of subsequently transplanted donor-type heart allografts in the absence of direct allorecognition of donor MHC class II molecules. BALB/c mice were treated with a portal injection of either irradiated (30 Gy) allogeneic C2D or WT B6 splenocytes (30×10^6), and the donor-type heart allografts were subsequently transplanted 7 days later. **A**, Survival curves of WT heart allografts. Five untreated BALB/c mouse recipients were used as controls (dotted line), and five BALB/c mouse recipients were treated with a portal injection of irradiated B6 splenocytes (solid line). $p < 0.01$, untreated control BALB/c mice vs BALB/c mice treated with a portal injection of irradiated B6 splenocytes. **B**, Survival curves of C2D heart allografts. A portal injection of B6 C2D splenocytes prolonged the survival of subsequently transplanted heart allografts. Four untreated BALB/c mouse recipients were used as controls (dotted line), and five BALB/c mouse recipients were treated with a portal injection of irradiated B6 C2D splenocytes (solid line). $p < 0.01$, untreated control BALB/c mice vs BALB/c mice treated with a portal injection of irradiated B6 C2D splenocytes.

B6 splenocytes, even when both the splenocytes infused and the heart allograft lacked MHC class II molecules (data not shown). These findings indicate that the portal injection of irradiated allogeneic splenocytes in fact did not induce a long-lasting tolerance state in T cells and that the indefinite acceptance of the heart allograft resulting from the portal injection of irradiated allogeneic splenocytes might be derived from mechanisms other than persistent T cell tolerance.

LSECs actively endocytosed allogeneic splenocytes injected via the portal vein

It could be possible that LSECs play a role in the immune regulatory effects induced by a portal injection of allogeneic cells on T cells with indirect allospecificity, regardless of the relevance of their role in the acceptance of subsequently transplanted heart allografts. It has been reported that LSECs show a large endocytic capacity for many ligands, including glycoproteins, components of the extracellular matrix, immune complexes, transferrin, and ceruloplasmin (33–37); however, further studies are required to elucidate whether LSECs endocytose allogeneic splenocytes after

portal venous injection. For this purpose, we isolated CD105⁺ cells from BALB/c mice treated with a portal injection of irradiated B6 C2D splenocytes. The sorted CD105⁺ cells always contained >95% of CD11b⁻ cells that had taken up Ac-LDL-BODIPY; these stained cells represented LSECs (Fig. 2A). We also confirmed that the isolated CD105⁺ cells were completely free of contamination with CD45⁺ hemopoietic cells, which might have the capacity for Ag presentation. B6 C2D splenocytes were labeled with PKH26 before portal injection to identify the LSECs that endocytose the injected splenocytes as PKH26-labeled cells.

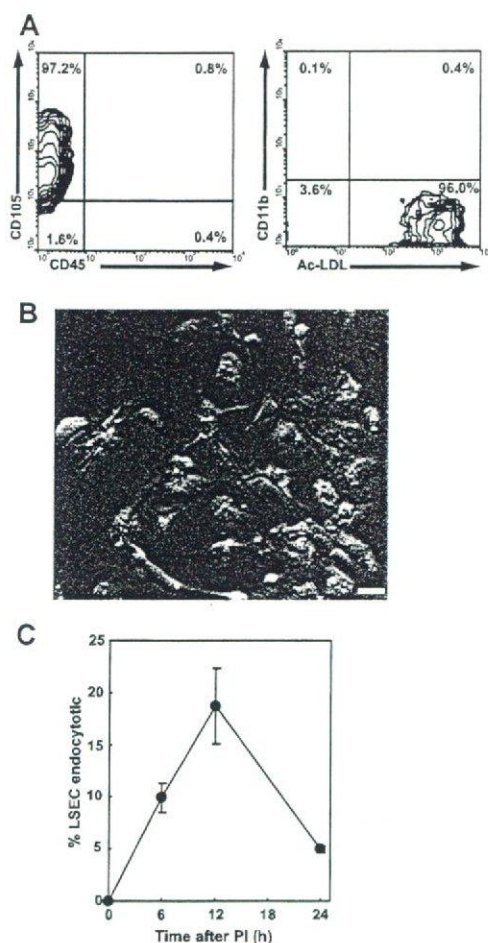


FIGURE 2. LSECs actively endocytosed allogeneic splenocytes injected via the portal vein. **A**, Purity of isolated LSECs. The nonparenchymal cell fraction obtained from the liver of BALB/c mice that were either untreated or treated with a portal injection were stained with anti-CD105 mAb and sorted by an autoMACS cell sorter. To analyze the purity of LSECs, the sorted CD105⁺ cells were stained with anti-CD45 FITC (30F11.1) to detect the expression of CD45 as a marker for hemopoietic cells (*left panel*). Aliquots of the sorted fractions were cultured in the presence of Ac-LDL-BODIPY for 12 h, and the sorted cells were stained with anti-CD11b PE (M1/70) to detect the expression of CD11b as a marker for Kupffer cells (*right panel*). Representative FCM profiles are shown. The percentages indicate the total sorted CD105⁺ cells. **B**, The relief confocal microscopy image of CD105⁺ LSECs isolated from the host liver 12 h after the portal injection of irradiated B6 C2D splenocytes by positive selection using an autoMACS cell sorter (scale bar, 20 μ m). B6 C2D splenocytes were labeled with PKH26 before portal injection into the BALB/c mice to identify the LSECs that had endocytosed the injected splenocytes as PKH26-labeled cells (red). **C**, Kinetics of the uptake of allogeneic-irradiated B6 C2D splenocytes by LSECs were analyzed by FCM. The percentages of PKH26-labeled phagocytic LSECs are shown for CD105⁺ cells isolated from the host liver.

Microscopic observation of the intracytoplasmic staining with PKH26 ruled out the possibility of the occurrence of doublets of LSECs along with adherents of the injected splenocytes or fragments (Fig. 2B). At 12 h after the portal injection, ~20% of LSECs had endocytosed the PKH26-labeled splenocytes (Fig. 2C). In the phenotypic analyses, LSECs from untreated mice expressed low amounts of MHC class II, CD40, CD80, and CD86 phenotypes; these are surface molecules necessary for the efficient Ag presentation to T cells. LSECs that endocytosed the irradiated allogeneic splenocytes showed enhanced expression of MHC class II molecules and CD80, indicating their capacity for Ag presentation to CD4⁺ T cells (Fig. 3). Notably, such LSECs concurrently lost CD40 expression and up-regulated FasL expression on their surface, suggesting the tolerogenic potential of the LSECs toward responding T cells.

Induction of specific unresponsiveness in T cells with indirect allospecificity by transmigration across autologous LSECs that had endocytosed allogeneic splenocytes

The various functions of APCs (professional myeloid APCs) such as uptake, processing, and presentation of Ags are temporally and spatially separated. APCs endocytose peripheral Ags and then undergo maturation during their migration into the lymphatic tissue, where they encounter T cells in a specialized microenvironment. The LSEC has been described as a new type of organ-resident APC that executes all three salient functions of an APC simultaneously and exhibits immunomodulatory activity toward naive T cells (17, 18). It is possible that LSECs process the endocytosed allogeneic splenocytes and subsequently present alloantigens to the naive T cells.

We examined the effect of Ag presentation by LSECs to naive T cells with indirect allospecificity on the responsiveness of these T cells to a subsequent alloantigen presentation by professional APCs. For this purpose, we performed a transendothelial migration assay to mimic the structural features of the interaction between LSECs and T cells. In the liver, blood passes through a meshwork of sinusoids formed by LSECs. Therefore, circulating leukocytes frequently come in contact with LSECs owing to the small diameter (7–12 μ m) of the sinusoids (38). Such a sinusoidal architecture is likely to promote the immunomodulatory activity of LSECs toward T cells. CFSE-labeled naive BALB/c nonadherent splenocytes first underwent transmigration across a monolayer (pores with a diameter of 8 μ m) of LSECs from BALB/c mice that were either untreated or treated with a portal injection of irradiated allogeneic B6 C2D splenocytes; this enabled direct interaction between T cells and LSECs (Fig. 4A). The transmigrated BALB/c lymphocytes were subsequently stimulated with splenic APCs from BALB/c mice that had been stimulated by treatment with an i.v. injection of the splenocytes from either donor-type B6 C2D or third-party C3H mice. The proliferative response of naive BALB/c CD4⁺ T cells to BALB/c APCs pulsed with B6 C2D splenocytes could be detected on FCM plots, although their stimulation indexes were lower than those usually observed in direct MLR assays in the fully allogeneic combinations. Such low stimulation indexes in indirect MLR assays are consistent with the previously reported fact that the frequency of T cells engaged in the indirect pathway of allorecognition is ~100-fold lower than that of T cells participating in direct recognition (39). The enhanced proliferative response of the presensitized BALB/c CD4⁺ T cells (prepared by B6 C2D skin grafting) to BALB/c APCs pulsed with B6 C2D splenocytes proved the suitability of this indirect MLR assay. Nonetheless, the CD4⁺ T cells that had transmigrated across the LSECs from mice that were treated with a portal injection of irradiated B6 C2D splenocytes lacked the proliferative response to BALB/c

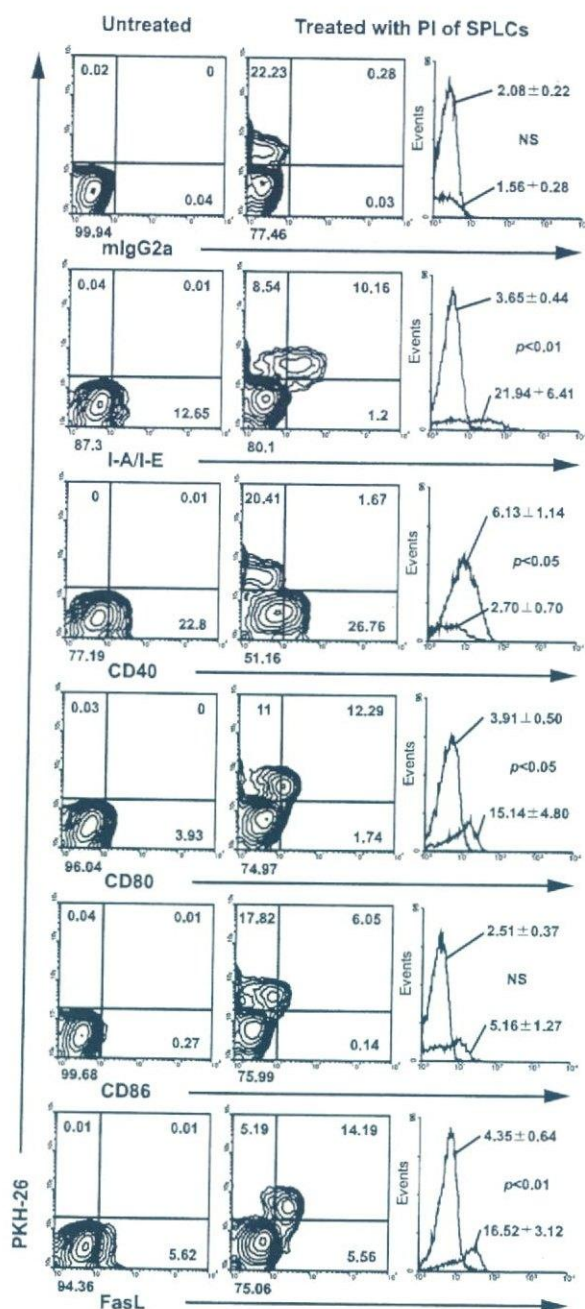


FIGURE 3. Phenotypic characteristics of LSECs that endocytosed allogeneic splenocytes. Host LSECs were isolated 12 h after a portal injection of irradiated B6 C2D splenocytes (30×10^6) labeled with PKH26 into BALB/c mice. These were stained with anti-mouse I-A/I-E FITC, anti-CD40 FITC, anti-CD80 FITC, and FasL mAb. The LSECs that had endocytosed the injected splenocytes could be identified as PKH26-labeled cells by FCM analysis. The percentage of total sorted CD105⁺ cells in each fraction are shown. PKH26⁺ LSECs and PKH26⁻ LSECs were selected by gating to compare the expression of various surface markers. The histogram reveals that PKH26⁺ LSECs (shaded histogram) expressed significantly higher levels of I-A/I-E, CD80, and FasL than the PKH26⁻ LSECs (solid line). PKH26⁺ LSECs lost CD40 expression on their cell surface. The expression levels of each marker are presented as median fluorescence intensity. Average values \pm SEM for the PKH26⁺ and PKH26⁻ LSECs are shown. FCM analysis using anti-CD105 mAb revealed that the inocula of splenocytes prepared from B6 mice did not include CD105⁺ cells (<0.5%) (data not shown). The FCM profiles are representative of four independent experiments.

APCs pulsed with B6 C2D splenocytes, while maintaining a normal response to BALB/c APCs pulsed with C3H splenocytes (Fig. 4, B and C). Thus, CD4⁺ T cells that transmigrated across the Ag-presenting LSECs that had endocytosed allogeneic splenocytes were rendered unresponsive to alloantigens via indirect recognition in an Ag-specific manner. The proliferative response of the BALB/c CD8⁺ T cells that transmigrated across the BALB/c LSECs to BALB/c APCs pulsed with B6 C2D splenocytes was undetectable even on FCM plots, regardless of whether pretreatment with a portal injection of B6 C2D splenocytes was conducted (data not shown). This might be attributed to the much lower number of CD8⁺ T cells with indirect allospecificity than those of CD4⁺ T cells with indirect allospecificity, as demonstrated previously (40).

Exposure to LSECs that endocytose alloantigens attenuated the IL-2-secreting activity of CD4⁺ T cells with indirect allospecificity

We have previously reported a method that combines MLR, which uses a CFSE-labeling technique, intracellular cytokine immunofluorescence staining, and multiparameter FCM analysis for the simultaneous determination of proliferation and cytokine-secreting activity of T cells responding to allostimulation (28). Using this technique, IL-2-secreting cells were detected in proliferating BALB/c CD4⁺ T cells in response to BALB/c APCs pulsed with B6 C2D splenocytes (Fig. 5). Transmigration across the LSECs from mice that were treated with a portal injection of irradiated B6 C2D splenocytes significantly reduced the frequency of IL-2-secreting cells in proliferating BALB/c CD4⁺ T cells in response to BALB/c APCs pulsed with B6 C2D splenocytes. In contrast, the frequency of the IL-2-secreting cells remained high in proliferating BALB/c CD4⁺ T cells in response to BALB/c APCs pulsed with C3H splenocytes. Thus, the exposure to LSECs that endocytose donor-type alloantigens attenuated not only the proliferating activity but also the IL-2-secreting activity of CD4⁺ T cells with indirect allospecificity.

CD4⁺ T cells that transmigrated across the LSECs that had endocytosed allogeneic splenocytes were rendered unresponsive to alloantigens by a mechanism involving Fas/FasL interaction

Based on the results of phenotypic studies showing enhanced expression of FasL on the LSECs that endocytose allogeneic splenocytes and the previously reported result that FasL engagement inhibits CD4⁺ T cell proliferation, cell cycle progression, and IL-2 secretion (41–43), we assumed that such LSECs inhibited allospecific T cell proliferation via apoptosis through Fas/FasL interaction. Consistent with this hypothesis, the transmigration of naive BALB/c CD4⁺ T cells across the LSECs from FasL-deficient BALB/c-*gld* mice treated with a portal injection of B6 C2D splenocytes failed to induce unresponsiveness in allospecific T cells (Fig. 6). This observation ruled out the possibility that the loss of ability of BALB/c CD4⁺ T cells to respond to BALB/c APCs pulsed with B6 C2D splenocytes was merely due to the adhesion of the responding BALB/c CD4⁺ T cells to LSECs.

Adaptive transfer of BALB/c LSECs that had endocytosed B6 C2D splenocytes into BALB/c mice via the portal vein prolonged the survival of subsequently transplanted B6 C2D hearts

Next, we investigated the biological significance of the mechanism of LSECs that was described earlier, and the relevance of such a mechanism with regard to the acceptance of heart allografts after a portal injection of allogeneic cells. LSECs obtained from BALB/c mice 12 h after the portal injection of irradiated B6 C2D

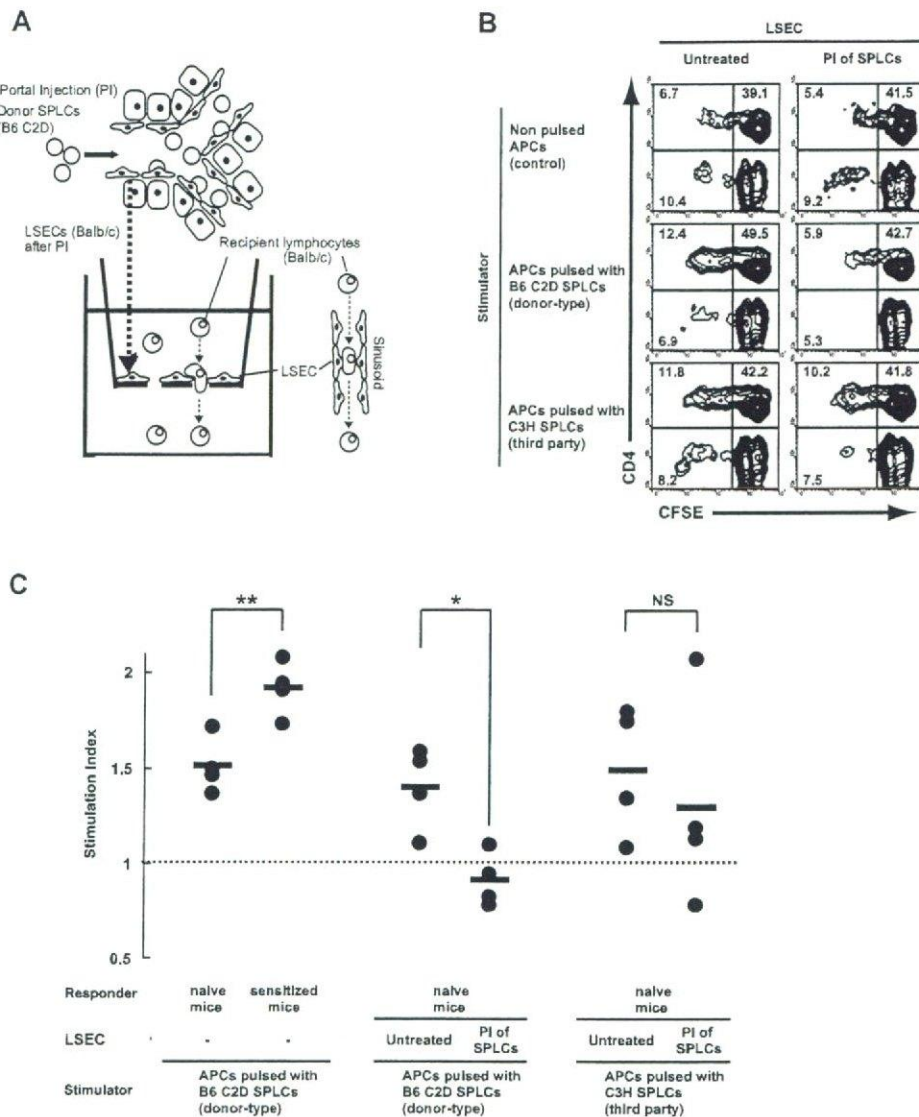


FIGURE 4. CD4⁺ T cells with indirect allospecificity were rendered unresponsive to alloantigens on contact with autologous LSECs that had endocytosed the respective alloantigens. **A**, System of transendothelial migration assay. Seven days after the portal injection, the LSECs were isolated from BALB/c mice that were either untreated or treated with a portal injection of irradiated allogeneic B6 C2D splenocytes. The isolated LSECs were applied onto the cell culture insert of a polycarbonate filter that was fibronectin-coated and had a pore size of 8 μ m. After 12 h of culture, the nonadherent cells were removed from the polycarbonate filter membrane by washing. CFSE-labeled naive BALB/c nonadherent splenocytes first underwent transmigration across a monolayer of LSECs from BALB/c mice that were either untreated or treated with a portal injection of irradiated allogeneic B6 C2D splenocytes; this enabled direct interaction between T cells and LSECs. The transmigrated BALB/c lymphocytes were subsequently stimulated with splenic APCs from BALB/c mice that had been treated with an i.v. injection of splenocytes from either donor-type B6 C2D or third-party C3H mice (indirect MLR). CFSE-labeled responder cells (2×10^6) were cultured with 4×10^5 irradiated stimulator cells in the ratio of 5:1 for 5 days. After the indirect MLR, the harvested lymphocytes were stained with PE-conjugated anti-mouse CD4 mAb. Subsequently, T cell proliferation (division) was visualized by FCM analysis as the serial halving of CFSE-fluorescence intensity. **B**, Representative FCM results of CFSE-labeled CD4⁺ T cell division in the subsequent indirect MLR. **C**, Stimulation indexes of CD4⁺ T cells with indirect allospecificity in the subsequent indirect MLR are shown. Each point represents an individual mouse, and the average values of four independent mice in each group are shown. *, $p < 0.05$; **, $p < 0.01$.

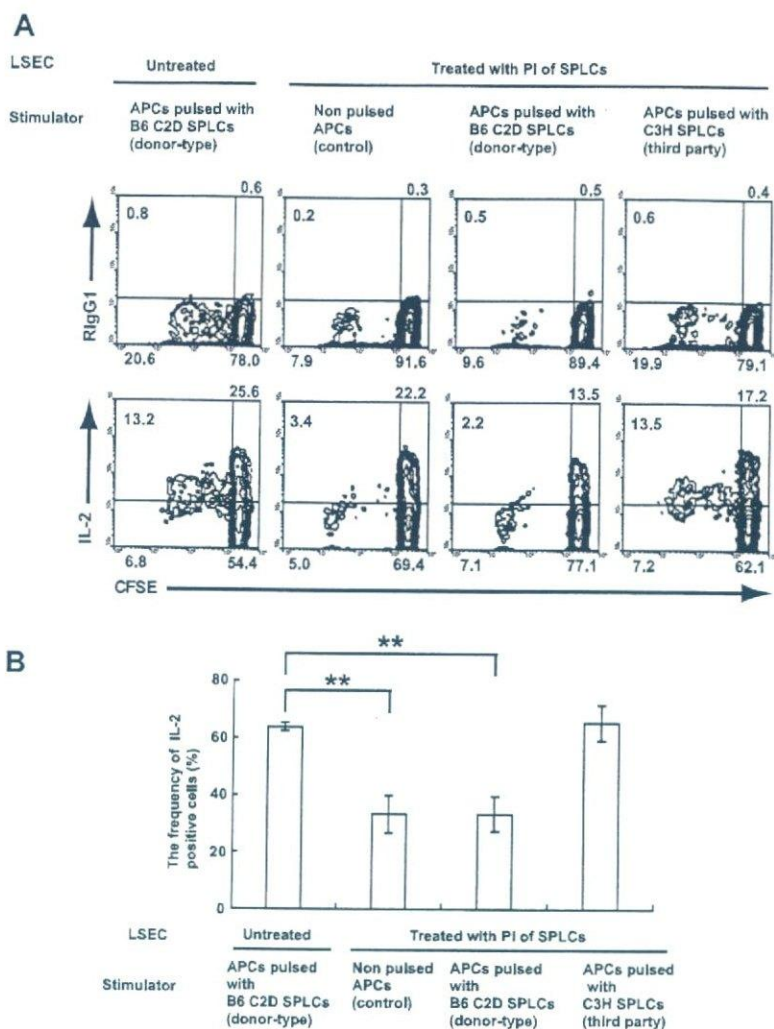
splenocytes were adaptively transferred via the portal vein into BALB/c mice (2×10^6 cells/mouse). After 7 days, allograft hearts from B6 C2D mice were transplanted into BALB/c mice. Adaptive transfer of LSECs from BALB/c mice treated with a portal injection of irradiated B6 C2D splenocytes prolonged the survival of subsequently transplanted allograft hearts, although this effect was not long lasting. The prolonging effect of adaptive transfer of LSECs from BALB/c-*gld* mice treated with a portal injection of irradiated B6 C2D splenocytes on the survival of subsequently transplanted allograft hearts was significantly less than that of LSECs from WT BALB/c mice treated similarly (Fig. 7). Thus, the

immunosuppressive effect of LSECs on T cells with indirect allospecificity via the Fas/FasL pathway is involved in the mechanism underlying the prolongation of heart allograft survival after a portal injection of allogeneic cells, at least in the early phase.

Discussion

The liver appears to favor the induction of immune tolerance rather than immunity. A number of observations demonstrate that Ag-specific immune tolerance is the result of Ag presentation in the liver. Allogeneic liver transplants are often well accepted by a recipient (44–46), leading to tolerance to further organ transplants

FIGURE 5. Exposure to LSECs that endocytose alloantigens attenuated the IL-2-secreting activity of CD4⁺ T cells with indirect allospecificity. The transigrated BALB/c CFSE-labeled responder lymphocytes were cultured with irradiated stimulator splenic APCs from BALB/c mice that had been stimulated with an i.v. injection of splenocytes from either donor-type B6 C2D or third-party C3H mice. The indirect MLR-cultured cells were stained with PerCP-Cy5.5-conjugated anti-CD4, followed by staining with allophycocyanin-conjugated annexin V. Subsequently, the cells were fixed, permeabilized, and stained with PE-conjugated IL-2 mAbs or isotype-matched control Abs (IgG1). A four-colored FCM was performed to determine the proliferation and cytokine-secreting activity in the MLR. CD4⁺ T cells were selected by gating and analyzed for IL-2-secreting activity. **A**, Representative FCM results of CFSE-labeled CD4⁺ T cell division in the indirect MLR. The FCM profiles shown are representative of four independent experiments. The number refers to the percentage of total cells in each quadrant. **B**, The frequency of IL-2-producing cells in the proliferated CD4⁺ T cell fractions. The frequency (%) was calculated using the quadrant data of the FCM contour plots in **A** according to the following formula: percentage of the upper left/(percentage of the upper left + percentage of the lower left) × 100. Average values ± SEM for four independent experiments are shown. **, $p < 0.01$.



from the same donor but not to third-party grafts (47, 48). We have recently demonstrated a novel relevant mechanism of such liver allograft tolerance, i.e., naive allogeneic LSECs selectively tolerize CD4⁺ and CD8⁺ T cells with direct allospecificity in mice in which liver allografts are normally accepted without recipient immune suppression across MHC barriers (49). In allogeneic mixed hepatic constituent cell-lymphocyte reaction (MHLR) assay, whole constituent cells did not promote T cell proliferation. When LSECs were depleted from the hepatic constituent cell stimulators in the allogeneic MHLR assay, a marked proliferation of reactive CD4⁺ and CD8⁺ T cells was observed. After restimulation with irradiated BALB/c splenocytes, we observed nonresponsiveness of B6 T cells that had transigrated across allogeneic BALB/c LSECs and marked proliferation of T cells that had transigrated across syngeneic B6 or third-party SJL/j LSECs. These results raised the question of whether a similar mechanism involving LSECs can explain another well-known phenomenon of increased graft acceptance after a pretransplant portal venous injection of donor leukocytes (3, 4).

The LSEC has been described as a new type of APC that induces immune tolerance in naive T cells (17, 18). Furthermore, LSECs are capable of stimulating naive CD4⁺ T cells. However, following priming by Ag-presenting LSECs, CD4⁺ T cells fail to subsequently differentiate into Th1 phenotype, instead they differentiate into regulatory T cells that express IL-4 and IL-10 on restimulation (6, 50). LSECs also have the capacity to present

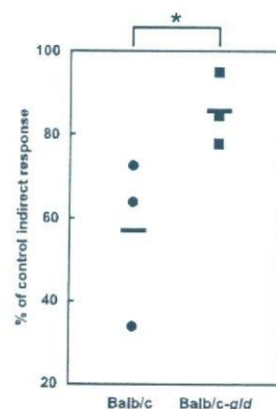


FIGURE 6. CD4⁺ T cells that transigrated across the LSECs that had endocytosed allogeneic splenocytes lost their responsiveness to alloantigens by a mechanism involving Fas/FasL interaction. CFSE-labeled BALB/c splenocytes first underwent transmigration across the LSECs from BALB/c WT (●; $n = 3$) or BALB/c-gld FasL-deficient mice (■; $n = 3$) that were treated with a portal injection of irradiated B6 C2D splenocytes. The transigrating cells were subsequently stimulated with the irradiated splenic APCs from BALB/c mice that had been pulsed with an i.v. injection of donor-type B6 C2D splenocytes (indirect MLR). The inhibition rate of indirect alloimmune response by the LSECs was represented by the percentage of stimulation index of CD4⁺ T cells transigrating across the LSECs from the untreated control BALB/c mice. *, $p < 0.05$.

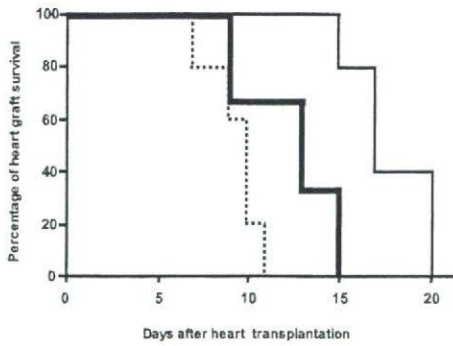


FIGURE 7. Adaptive transfer of BALB/c LSECs that had endocytosed B6 C2D splenocytes into BALB/c mice via the portal vein prolonged the survival of subsequently transplanted B6 C2D hearts. LSECs were obtained from either untreated BALB/c mice, BALB/c mice 12 h after a portal injection of irradiated (30 Gy) B6 C2D splenocytes (30×10^6 cells/mouse), or BALB/c-*gld* FasL-deficient mice 12 h after a portal injection of irradiated B6 C2D splenocytes. The isolated LSECs were adaptively transferred via the portal vein into BALB/c mice (2×10^6 cells/mouse), and the allograft hearts from B6 C2D mice were transplanted 7 days later. Survival curves of B6 C2D heart allografts are shown. Five BALB/c mice received untreated BALB/c LSECs (dotted line), five BALB/c mice received BALB/c LSECs that had endocytosed B6 C2D splenocytes (solid line), and three BALB/c mice received BALB/c-*gld* LSECs that had endocytosed B6 C2D splenocytes (bold line). $p < 0.01$, recipients of untreated BALB/c LSECs vs those of BALB/c LSECs that had endocytosed B6 C2D splenocytes. $p < 0.02$, recipients of BALB/c LSECs that had endocytosed B6 C2D splenocytes vs those of BALB/c-*gld* LSECs that had endocytosed B6 C2D splenocytes.

exogenous Ags on MHC class I molecules to CD8⁺ T cells, a process termed as cross-presentation (5). Initially, the stimulation of naive CD8⁺ T cells by LSECs results in the proliferation of T cells and the release of cytokines. However, finally, it leads to Ag-specific tolerance, as demonstrated by the simultaneous loss of cytokine expression and the failure of CD8⁺ T cells to develop into cytotoxic effector T cells. However, such immune regulatory effects of LSECs have been observed only in a model in which the interaction of soluble exogenous Ags and its corresponding transgenic TCRs occurs. Thus, the capacity of LSECs to regulate a polyclonal population of nontransgenic T cells with allogeneic specificity remains to be elucidated.

We demonstrated that host LSECs actively endocytose allogeneic splenocytes injected via the portal vein. Host LSECs that endocytose allogeneic splenocytes highly expressed MHC class II molecules and CD80 costimulatory molecules, probably due to the processing of endocytosed allogeneic cells and presentation of alloantigens. It is possible that the LSECs process the endocytosed allogeneic splenocytes and subsequently present alloantigens to naive CD4⁺ T cells through interaction between autologous MHC class II molecules and TCRs. Such Ag presentation by LSECs might negatively regulate CD4⁺ T cells with indirect allospecificity. The cumulative surface area of LSECs is very large, and hepatic microcirculatory parameters allow frequent contact between LSECs and passenger leukocytes. Considering the large volume of blood that passes through the liver daily, it is probable that LSECs are ideally positioned within the liver to establish peripheral immune tolerance (17, 51). We conducted a T cell transendothelial migration assay to mimic the structural features of the interaction between LSECs and T cells. In this system, the responsiveness of naive CD4⁺ T cells to stimulus with syngeneic splenic APCs pulsed with allogeneic C2D splenocytes was abrogated by transmigration across LSECs that endocytosed allogeneic C2D splenocytes;

this indicates that T cells with indirect allospecificity could be negatively regulated by direct contact with LSECs that present alloantigens (Fig. 4). We also demonstrated that the up-regulation of FasL expression on LSECs that endocytosed allogeneic cells could contribute to their immunosuppressive potential on alloantigen recognition via the indirect pathway. The deficiency of FasL on LSECs in mutant mice significantly attenuated their suppressive property toward CD4⁺ T cells with indirect allospecificity (Fig. 6). Because there appears to be a residual inhibitory effect of LSECs on T cells even in the absence of FasL, mechanisms other than the Fas/FasL pathway may also be involved in the LSEC-induced immunosuppression of CD4⁺ T cells. Based on the previously reported results demonstrating the importance of CD40/CD154-mediated costimulation in indirect presentation models (52, 53), insufficient expression of costimulatory molecules, i.e., significant down-regulation of CD40 expression on the LSECs that endocytosed allogeneic cells (Fig. 3), might contribute to their immunosuppressive effects.

Endothelial cells have been shown to activate T cell responses toward alloantigens, thereby triggering transplant rejections (54). However, recently, it has been reported that endothelial cells exposed to IL-10, IFN- α , and/or vitamin D3 induce the expression of Ig-like transcript (ILT)3 in endothelial cells, thereby tolerizing them (55). ILT3 belongs to a family of Ig-like inhibitory receptors that are structurally and functionally related to killer cell inhibitors and contains ITIMs (56–58) that mediate the inhibition of cell activation by recruiting tyrosine phosphatase Src homology protein-1 (57). Because various hemopoietic cells (i.e., intrahepatic macrophages, dendritic cells, NK cells, NK T cells) that reside in the liver have a capacity to release anti-inflammatory mediators, including IL-10, the expression of ILT3 in LSECs might be induced by factors unique to the liver microenvironment. The possibility of such an alternative explanation for LSEC-induced immunosuppression of T cells with indirect allospecificity remains to be elucidated.

In this study, although we proved that T cells with indirect allospecificity lose their reactivity on exposure to LSECs that endocytose alloantigens, at least partially through Fas/FasL interaction, the relevance of such a mechanism with regard to the acceptance of heart allografts after a portal injection of allogeneic cells remains unclear. The adaptive transfer of BALB/c LSECs that had endocytosed B6 C2D splenocytes into BALB/c mice prolonged the survival of subsequently transplanted B6 C2D hearts; however, this effect was not long lasting. This indicates that the immunosuppressive effect of LSECs on T cells plays a significant role at least in the early phase after the portal injection of allogeneic cells. However, further investigations are required to clarify the responsibility of LSECs for persistent acceptance of heart allografts after a portal injection of allogeneic cells. In the present study, MHC class II-deficient heart allografts appeared to be more susceptible to persistent acceptance induced by a portal injection of allogeneic cells than MHC class II-expressing heart allografts. It is possible that the immunosuppressive effect of the portal injection of donor cells is more efficient in T cells with indirect allospecificity than in T cells with direct allospecificity. Alternatively, it is also possible that grafts that do not express MHC class II molecules merely survive longer than grafts that express these molecules. In either case, the influence of a portal injection of donor cells on T cells with direct allospecificity remains to be elucidated. Previous studies have shown a prolonged allograft survival after an intrathymic injection of donor MHC peptides. This suggests that the manipulation of the indirect pathway can alter the course of rejection when both direct and indirect responses are available (59, 60);